AD-A045 666 GENERAL ELECTRIC CO SYRACUSE N Y ELECTRONICS LAB F/G 17/1
THE APPLICATION OF HOLOGRAPHIC CONCEPTS TO SONAR,(U)
APR 69 W A PENN, J L CHOVAN
UNCLASSIFIED R69ELS-48 NL

1 OF 1
AD
A045666

END
DATE
FILMED
11-77
DDC

| OF |

AD
A045666

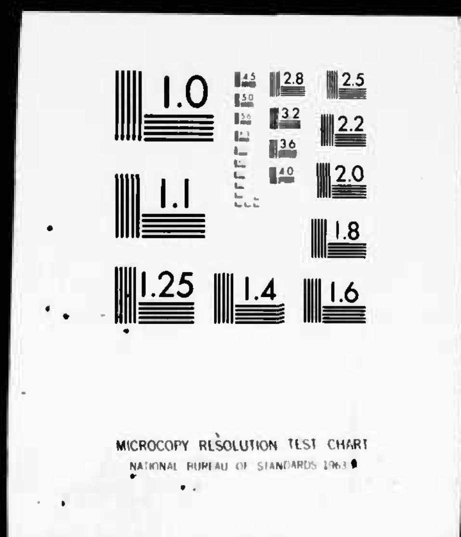

ADA045666

MOST Project -12

ELECTRONICS LABORATORY • SYRACUSE, N.Y.

MOST Project -12

(10) (14) (11) (6) (12)

AUTHOR	SUBJECT	NO.
W.A. Penn J.L. Chovan	Acoustical Holography, Sonar	R69ELS-48
		DATE Apr 1969
TITLE THE APPLICATION OF HOLOGRAPHIC CONCEPTS TO SONAR		GE CLASS 1
		GVT CLASS None
REPRODUCIBLE COPY FILED AT TECHNICAL INFORMATION EP13	ELECTRONICS LABORATORY SYRACUSE, N.Y.	NO. OF PAGES 59

24 p.

SUMMARY

This material was presented as a paper to the 2nd International Symposium on Acoustical Holography sponsored by McDonnell-Douglas at Huntington Beach, California, March 6, 1969.

The possible application of acoustical holography to conventional sonar problems is considered, in which acoustical fields are recorded in optical form and optically reconstructed. Also considered are other related coherent optical techniques for processing sonar data.

The similarities, differences, and limitations of the various systems are described. Comparisons are made which include: ranging and lateral resolution, aperture size, number of array elements, bandwidth, center frequency, and the possibility of signal averaging to improve image quality.

KEY WORDS Holography, Signal Processing, Sonar, Acoustics, Optics

INFORMATION PREPARED FOR Electronics Laboratory, Heavy Military Electronic Systems

WORK CONDUCTED BY Authors

APPROVED William A Penn (Sub Mgr) Charles G. Schnorr (Sect Mgr)

409508

THE APPLICATION OF HOLOGRAPHIC CONCEPTS TO SONAR

W. A. Penn, J. L. Chovan, General Electric Electronics Laboratory

The conventional signal processing and beamforming tasks that must be performed in a sonar system are traditionally accomplished by electronic analogue and digital means. Conceptually, these signal processing tasks can be very conveniently accomplished with optical systems, although then the required accompanying optical input recording process is usually a practical difficulty.

From another point of view, the process of acoustical holography, with optical reconstruction, can be used as a sonar device, i.e., to see objects in water.

These two conceptual approaches to sonar have much in common, and are both subject to several fundamental limitations. An important difference between them is the pulse echo-timing ability of conventional sonar, where range information is implied by echo delay, vs the CW nature of a holographic system, where range is obtained by parallactic or focusing effects. Hybrid systems are possible which incorporate the attributes of both approaches.

In this paper, the main features and basic limitations of the various possible systems which have been considered in this investigation are described, as well as the similarities and differences between them. Comparisons are made in terms of various trade-offs which include: ranging and lateral resolution, aperture size, number of array elements, bandwidth, center frequency, and the possibility of signal averaging to improve image quality.

TABLE OF CONTENTS

I. INTRODUCTION

The now extensive study of acoustical holography has indicated three important conceptual approaches to the process of sensing the acoustical wavefront, so that the resulting information can be used to form a hologram which can be reconstructed, usually by optical means. These approaches are:

1) The use of a continuous 2-dimensional recording medium, which then itself becomes the optical modulator, such as in the liquid-air or liquid-plastic techniques.

2) The use of a two-dimensional acoustically sensitive medium which must be scanned, such as in the Sokoloff tube, or a single acoustic sensor which is mechanically scanned. The result is thus obtained as scanned "video" information which must be recorded to form a holographic optical modulator.

3) The use of a matrix or array of acoustic sensors whose outputs are individually applied to corresponding points in an optical modulator to create a hologram. This may be accomplished sequentially by a commutating system, in which case the output actually obtained resembles scanned information.

The latter two approaches are amenable to the electronic insertion of the reference beam.

In light of this variety of possible techniques, a question which then suggests itself is whether any of them can be used to implement an acoustic viewing system in what is usually regarded as a sonar environment. That is, can a holographic system be used to advantage to replace present "conventional" sonar systems?

II. PRESENT PRACTICE IN SONAR PROCESSING

To answer this question, it is instructive to consider briefly and generically some of these presently existing or conceived sonar systems. Until now these systems have been relatively long range (hundreds of meters and up), but the intent here is not to exclude possible applications at shorter ranges (on the order of several meters).

In early sonar systems, the receiving antenna has been mechanically steered, and the receiver had essentially no signal processing, i.e., the received sounds were directly listened to by an operator. In modern systems, there is a strong tendency toward the use of acoustical phased arrays, and more sophisticated signal processing and display. Often coded pulses are transmitted, which must then be matched or compressed by the receiver. The received echoes may then be presented in form analogous to radar, in which echo delay or range is indicated as one display coordinate, and doppler frequency shift or received azimuth angle may be displayed along the other coordinate.

Operating frequencies, as a result of the intent of long range, have been generally in the region of several hundred cycles per second to the region of 100 kHz. In some short range systems the frequency may even exceed this. The region of 1-5 kHz is a very popular range for long range sonar. These considerations simply result from the conflicting desires to use a low frequency to avoid propagation losses, which become very important at long ranges, and to use a high frequency to enhance the angular resolution of the system with a reasonably sized array.

Figure 1 shows the attenuation characteristic of sea and fresh water. The loss in db/unit distance and the frequency are both plotted logarithmically. The inflection point occurs at a frequency of several hundred kHz, exhibiting an attenuation there of something less than 100 db/kilometer. At 5 kHz the losses have fallen to something like 0.1 db/Km.*

*This information is covered in detail in R. J. Urick, "Principles of Underwater Sound for Engineers", McGraw-Hill, 1967. (Reference 3)

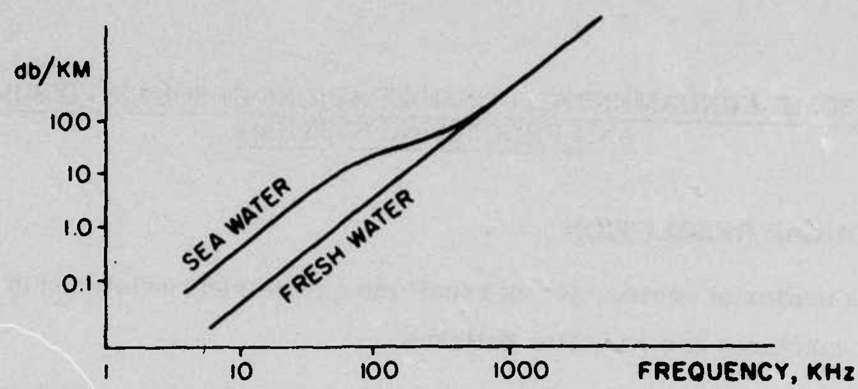

Figure 1. Water Propagation Loss

As will be discussed, it is necessary to use higher system bandwidths, if the range resolution is increased. If the resolution is increased to the point that a range resolution cell is equivalent to the size of the sonar array, beyond this point time-delay steering must be used if the beams are to be electronically steered. This is usually a more difficult task than phase-delay steering, which can be used at lower bandwidths. Many of the following techniques which will be described here assume that a phased array is appropriate and sufficient.

If a receiving array of hydrophones is used, the shape of the array may assume a variety of forms. It may be planar, cylindrical (with a vertical cylindrical axis), spherical, or "conformal", which means that the array conforms in shape to the vessel, i.e., the shape of the hull. Array elements are usually spaced in the region of 1/3 or 1/2 the wavelength to avoid array echelon or ambiguous beams. Thus, the element spacing is found to be in the range of several cm to nearly 1 meter. Beamwidths down to the region of several degrees have been achieved with array widths up to the region of 100 λ.

III. SOME FUNDAMENTAL CONSIDERATIONS IN SONAR VIEWING AND PROCESSING SYSTEMS

A. ANGULAR RESOLUTION

As a matter of review, let us recall the geometrical relationship between apertures and radiation patterns.

The angular resolution obtainable with a receiving array is related to the array in the same way whether one is considering microwaves, acoustics, or optics. The angular resolution, $\Delta\theta$, is approximately expressed in one dimension as

$$\Delta\theta = \frac{\lambda}{D} \tag{1}$$

where

λ = wavelength

D = array length

The specific example of a uniformly weighted array is usually used, where the far-field amplitude beam pattern is given as a function of the field angle θ:

$$A(\theta) = K \frac{\sin\left(\pi \frac{\theta D}{\lambda}\right)}{\left(\pi \frac{\theta D}{\lambda}\right)} \tag{2}$$

assuming small θ.

This results in a peak-to-first-null angular width of λ/D, a fact which can be reasoned rather directly from Figure 2. When the farfield angle is such that, due to the geometry, there is a spatial phase progression of exactly one cycle across the aperture, the coherent integration over this one cycle produces a zero result. This angle is geometrically recognized as approximately λ/D.

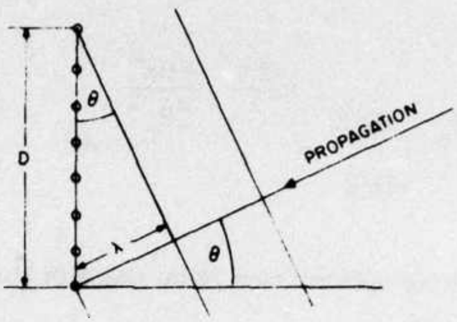

Figure 2. Angle of Arrival at Array

B. CW RANGING BY FOCUSSING OR PARALLACTIC EFFECTS

In a similar way, other phase errors, such as the approximately quadratic error due to a focal mismatch, became significant when their effect amounts to a phase shift of the order of one cycle across the aperture.

The specific case of a one-dimensional uniformly weighted aperture which is focussed on a point is shown in Figure 3. The proportional amplitude of radiation is found approximately by integrating along the aperture, observing the phase retardation as a function of aperture location:

$$A(\Delta R) = \int_{-D/2}^{+D/2} e^{j \frac{2\pi}{\lambda} R(x; \Delta R)} dx \tag{3}$$

where

$$\begin{aligned} R(x; \Delta R) &\cong R_o + \Delta R(1 - \cos\theta) \\ &\cong R_o + \Delta R \cdot \frac{\theta^2}{2} \cong R_o + \Delta R \frac{x^2}{2R_o^2} \end{aligned} \tag{4}$$

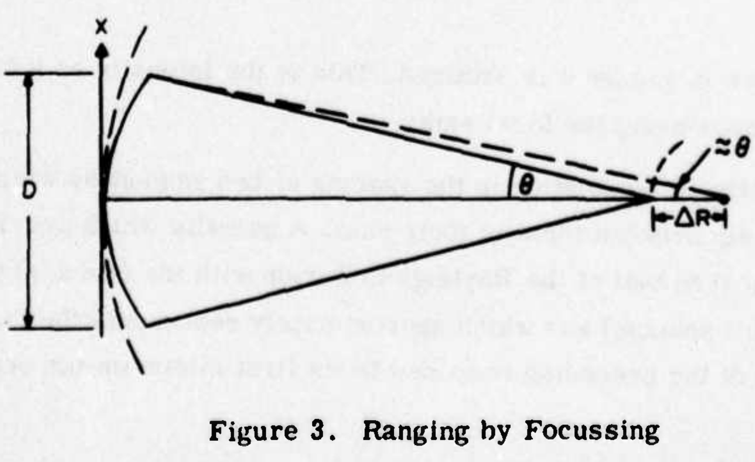

Figure 3. Ranging by Focussing

Thus,

$$A(\Delta R) = e^{j \frac{2\pi}{\lambda} R_o} \int_{-D/2}^{+D/2} e^{j \frac{2\pi}{\lambda} \frac{\Delta R x^2}{2 R_o^2}} dx \tag{5}$$

where

ΔR = Distance along optical axis from point of focus, R_o

D = aperture width

x = aperture coordinate

If we let

$$\left.\begin{aligned} \beta &= x \cdot \frac{1}{R_o} \cdot \sqrt{\frac{\pi \Delta R}{\lambda}} \\ \beta_a &= D/2 \cdot \frac{1}{R_o} \sqrt{\frac{\pi \, \Delta R}{\lambda}} \end{aligned}\right\} \tag{6}$$

Then the intensity or power at the measured point can be expressed as the square of (5) in the following form:

$$I = \left| K \int_{-\beta_a}^{+\beta_a} e^{j \beta^2} d\beta \right|^2 \tag{7}$$

which is recognized as a form of the Fresnel integral, and thus functionally well known.

If this intensity function is plotted vs. the normalized variable

$$\frac{\Delta R}{\left(\frac{R_o}{D}\right)^2 \lambda} = \frac{\Delta R}{(\text{optical "f -number"})^2 \cdot \lambda}$$

the result shown in Figure 4 is obtained. This is the intensity as a function of small distances along the focal axis.

One definition of resolution is the spacing of two responses which provides an acceptable dip between them in their sum. A quantity which provides a dip roughly equal to that of the Rayleigh criterion with the (sin x/x) form, (peak to 1st null spacing) and which approximately represents the distance from the peak of the preceding response to its first minimum (as seen from Figure 4) is

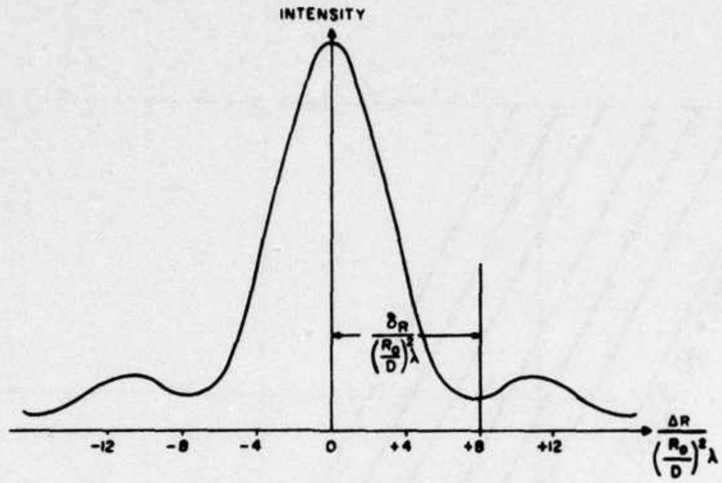

Figure 4. Variation of Intensity Along Optical Axis in Region of Focussed Spot (One-Dimensional Aperture)

$$\frac{\Delta R}{\left(\frac{R_o}{D}\right)^2 \lambda} = 8$$

Hence, we define a focal resolution quantity as

$$\delta_R = 8\left(\frac{R_o}{D}\right)^2 \lambda = 8\lambda \cdot (\text{optical f-number})^2 \tag{8}$$

The intensity associated with a 2-dimensional, square, uniformly weighted aperture, is proportional to the squared value of (7), and thus the resolution quantity expressed in (8) is still pertinent for this case.

All the foregoing can be compared with the intensity in a focussed region from a circular diffracting aperture, which is analyzed and plotted in Reference 1.* Here it is shown that the first minimum is located exactly at

$$\delta_R = 8\left(\frac{R_o}{D}\right)^2 \lambda$$

where D is now the aperture diameter.

For convenience, this result (apparently approximately valid for any reasonably shaped aperture in terms of its longest dimension) is plotted as a function of R/D and wavelength in Figure 5.

*Born and Wolf, Principles of Optics, p. 439. (Reference 1)

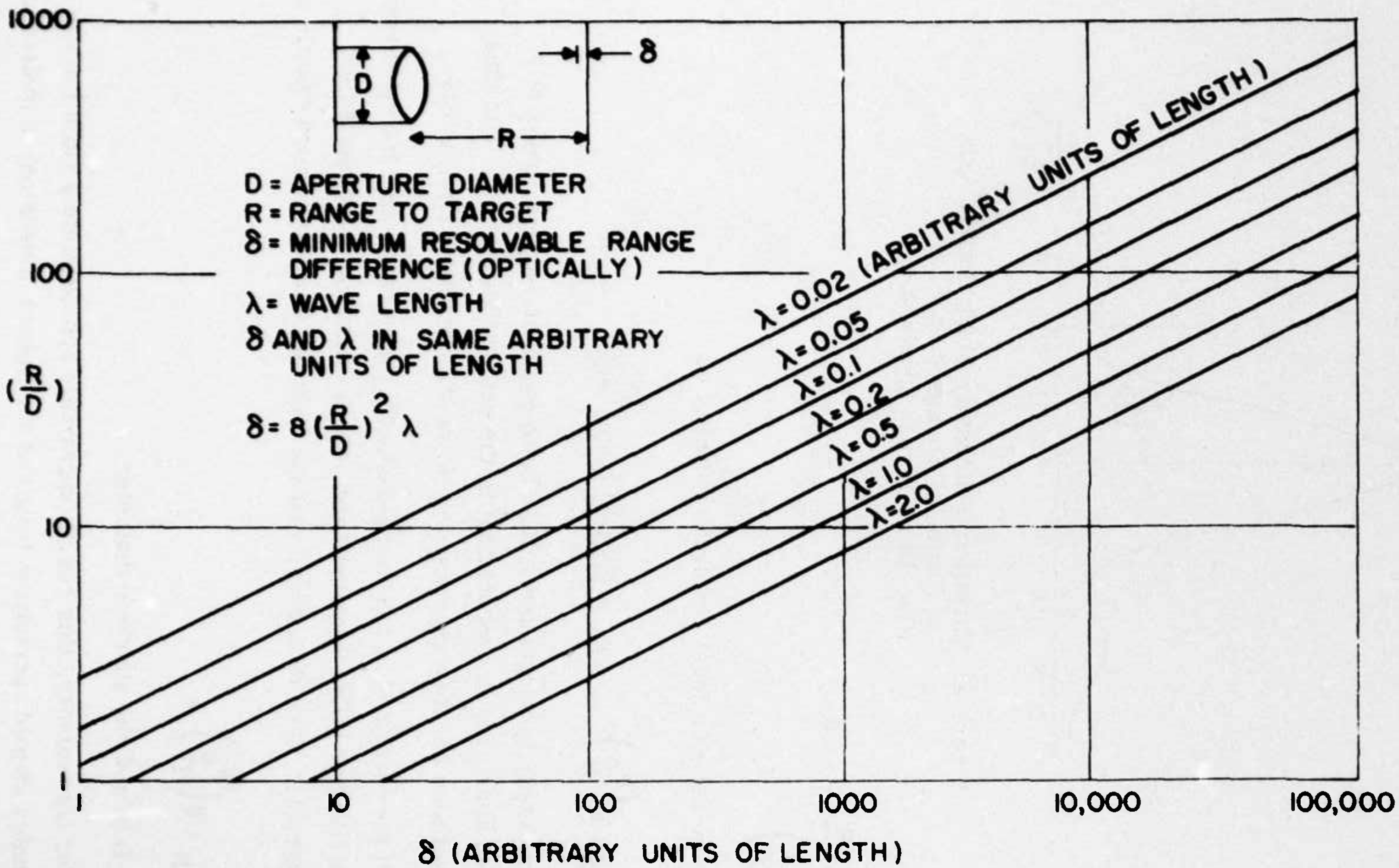

Figure 5. Range Resolution in CW Systems

As an example, let us assume a 100 kilohertz system, representing approximately a 15 mm wavelength. Assume a square array of 160,000 elements at $1/2\lambda$ spacing, i.e. 400 x 400. The aperture size would then be 3 meters on a side. Now consider the depth resolutions which would be associated with this system at the following ranges:

Range	Depth Resolution
3 meters	12 cm
30 meters	12 meters
300 meters	∞

The above example represents a very large number of elements, with a small wavelength, which is thus a very favorable example for depth discrimination, yet the performance collapses at reasonable ranges. Thus, it is obvious that, in general, for ranges that greatly exceed the array length, it is very difficult to obtain range measurements in this way.

C. RANGING BY ECHO TIMING

In light of the foregoing, one concludes that echo timing must remain the primary technique at high range resolution, and especially for sonar systems with low angular resolution, range discrimination is a source of important information. As is well known, the range resolution obtained with an echo timing system is given by:

$$\delta_R = \frac{c}{2\Delta f} \tag{9}$$

where

c = velocity of propagation

Δf = system bandwidth in cycles/time

The resolution is expressed in terms of bandwidth instead of pulse duration since in many cases a coded transmitted waveform is used instead of a simple pulse. In these cases the range resolution is determined by bandwidth.

Of many possible coded waveforms, the "chirp" or linearly frequency modulated pulse is the most popular in sonar systems. The chirp ambiguity diagram is shown in Figure 6.

The linear frequency sweep rate is given by ϵ, and Figure 6 depicts the fact that there is a range-doppler frequency ambiguity related by the

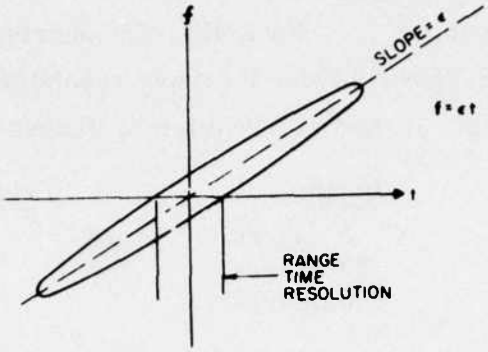

Figure 6. "Chirp" Pulse Ambiguity Function

coefficient ϵ. That is, if a target has a doppler frequency shift Δf_d, a matched receiver will register a range shift of $\Delta R = \frac{c\,\Delta f_d}{2\epsilon}$. Another code which is often considered is the pseudo-random phase code, which is free of range-doppler ambiguity.

To date, in sonar processors, coded waveforms have been compressed or matched by electronic analogue or digital means. The chirp waveform, however, is particularly adapted to coherent optical treatment, since the linear frequency variation is equivalent to a quadratic phase variation, i.e., $\phi = \pi \epsilon t^2$. In a coherent optical system, such a variation in phase can be matched by a focal shift. This, and optical techniques for processing other waveforms, will be considered in the next part of this discussion.

A limitation in pulse compression systems which must be kept in mind is a maximum allowable value of the waveform time-bandwidth product when a range of target velocities or doppler frequencies is expected. The difficulty can be thought of as the moving target passing out of a range resolution cell during the coded pulse duration. If the coded pulse duration is given by T, and the target velocity by v, we have from (9):

$$vT < \delta_R = \frac{c}{2\,\Delta f}$$

or $\quad \Delta f T = \text{time bandwidth product} < \frac{c}{2v}$ (10)

As an example, we might suppose the maximum target velocity to be expected in the water is 10 meters/sec. Then we find the upper time-bandwidth product which can be used is approximately 150.

D. NUMBER OF RESOLVABLE ELEMENTS AND FIELD OF VIEW

We next consider the possibility of using range discrimination together with the angular resolution capability of a linear hydrophone array to map out a picture, instead of the holographic technique of using two angular dimensions from a planar array. Also, let us suppose that under these conditions one would want an approximate match between range and azimuthal target dimension resolutions. From (1) and (9), this condition would be expressed as:

$$\frac{\lambda R}{D} = \frac{c}{2\Delta f}$$

$$\text{or} \quad \frac{R}{D} = \frac{f_o}{2\Delta f} = \frac{\delta_R}{\lambda} \tag{11}$$

where f_o = acoustic carrier frequency.

In words, we find that the ratio of range to aperture size must not be more than the reciprocal of the fractional bandwidth of the system.

Alternatively, one can say that if range resolution is matched to azimuthal resolution, the number of resolvable range cells is limited to approximately D/λ. This can be a significant limitation to matched range-azimuthal (or "PPI") pictures.

Again, considering the 100 kHz system, with a 3-meter aperture, matched resolution implies an upper limit of 200 range elements.

The same limitation exists for the number of azimuth elements, if the array has been designed to avoid ambiguities or echelon lobes.

If n linear elements are spaced by a distance d, a given phasing will cause two ambiguous beams θ_A apart, where θ_A is given for the symmetrical case by

$$2 \sin \frac{\theta_A}{2} = \frac{\lambda}{d} \tag{12}$$

which for small angles reduces to $\theta_A \cong \frac{\lambda}{d}$

The beam width is again given by (1):

$$\Delta\theta = \frac{\lambda}{D} = \frac{\lambda}{nd}$$

Thus, the total number of angle elements available between ambiguities is given by

$$N = \frac{\theta_A}{\Delta\theta} = n \qquad (13)$$

The total angle between ambiguities must be available, of course, and this will happen for element spacings down to $\lambda/2$, as shown in (12).

Thus the total number of resolvable angle elements (for 1 or 2 dimensions) is equal to the number of array elements for element spacings down to $\lambda/2$. Most sonar systems use $\lambda/2$ spacing, with slightly smaller spacing used in some cases to avoid endfire ambiguity.

In the case where received data is to be assembled into a hologram for viewing, the number of resolvable elements available in the hologram must exceed the number of field elements by at least a factor of 2, and usually somewhat more than this. This is due to the diffraction mechanism by which a hologram is reconstructed, where several carrier cycles must be recorded, whose positions are indicative of diffraction phase for each resolvable modulation or array element.

E. IMAGE QUALITY

In any coherent system in which an image is derived, there is a tendency for the image to suffer a multiplicative noise due to the random phase combination of returns from scatterers making up the object being viewed. If no averaging of independent images occurs, the statistical multiplicative function referred to is a Rayleigh amplitude distribution. This function is plotted in Figure 7. For this statistical behavior, it is found that the fluctuation amplitude is of the same order as the mean value.

A discussion of this theory is reviewed in Reference 8, and the effect of post detection averaging is discussed. It is shown that if P_a independent samples of the detected image is combined, the fluctuation noise is reduced by a factor $\sqrt{P_a}$. As the number of such independent samples becomes large, a smooth optical-like quality is obtained in the image.

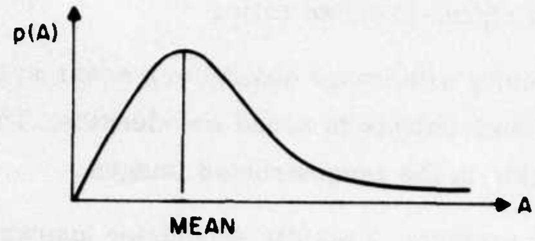

Figure 7. Rayleigh Probability Density

To achieve an independent sample of the image, all the phases of returns from the individual scatterers in a resolution cell must be relatively changed. This can be accomplished in several ways:

1. With a change of carrier frequency.
2. With motion of the scatterers.
3. With a shift of the viewing aperture equal to its own size.*

It is obvious that the latter variation can be accomplished by either moving the entire receiving array as specified, or by using equally sized subareas of the array sequentially. If, for example, the entire array is broken up into P_a subarrays, and the P_a independent images obtained from each are combined after detection, a decrease in fluctuation noise of $\sqrt{P_a}$ can be obtained.

Alternatively, one could use the entire array to obtain a high resolution picture with fluctuation. Then, photographically, or with a display mechanism, the resolution can be reduced by an area factor of P_a. This defocussing acts as the combining mechanism by which independent samples are averaged within the now larger resolution cell. The effect thus obtained is equivalent to the division of the array.

From the foregoing, it is apparent that there is a linear tradeoff between resolution (in area) and image averaging. Under certain conditions, a very small number of averaged images is sufficient to provide good quality, in which case it is worthwhile to sacrifice the modest amount of resolution required. These conditions are met when the image is properly

*See appendix in Reference 8.

compressed in dynamic range to match the available display range, and the image enjoys a high signal-to-noise ratio.

The other difficulty with image quality in a sonar system is the highly specular nature of most objects to sound wavelengths. This produces only thin lines of highlights in the reconstructed images.

To picture this problem, a plastic submarine approximately 1/3 meter in length was treated to be mirror-like or highly specular to visible light.* This model was then illuminated with laser light to simulate the fluctuation noise of a coherent system, and viewed through various pinholes to simulate various sizes of sonar arrays. It is felt that the resulting images are indicative of what can be expected with sonar holographic systems. In Figure 8, the viewing pinholes were the following sizes, which are felt to be typical of sonar arrays, in terms of wavelengths.

Figure 8-	Array Diameter
a)	Ordinary Optical image
b)	2000 λ (equivalent to 400 λ/θ subtended)
c)	800 λ (equivalent to 160 λ/θ subtended)
d)	200 λ (equivalent to 40 λ/θ subtended)

The angle subtended by the submarine from the viewing aperture is approximately 10°. The results are proportionally equivalent to smaller apertures at wider subtended angles. Thus we may say that the results are related to apertures as little as 1/5 the size actually used, in wavelengths, to larger values, depending on how close the object is.

On the left hand side of each picture is shown the result with a diffuse surface, which is equivalent to diffuse illumination (a wide source angle). On the right hand sides are shown the results with a specular surface, which is felt to be equivalent to the usual sonar situation.

---

*A silver-coated model would be ideal, but an equivalent specular achromatic behavior can be obtained with black glossy paint.

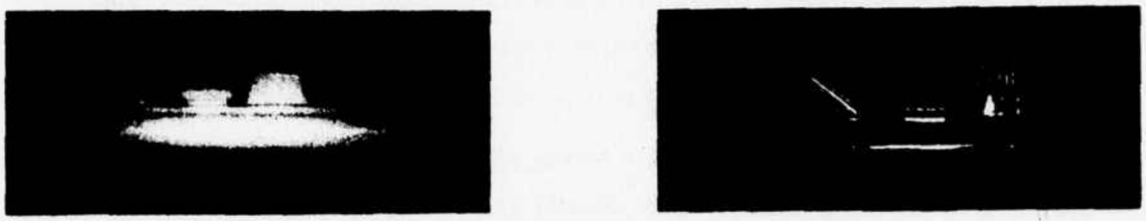

a) Ordinary Optical Image

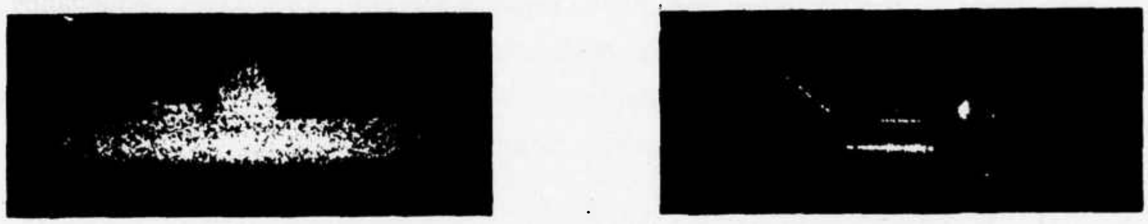

b) 2000 λ (equivalent to $\frac{400\ \lambda}{\theta_{subtended}}$)

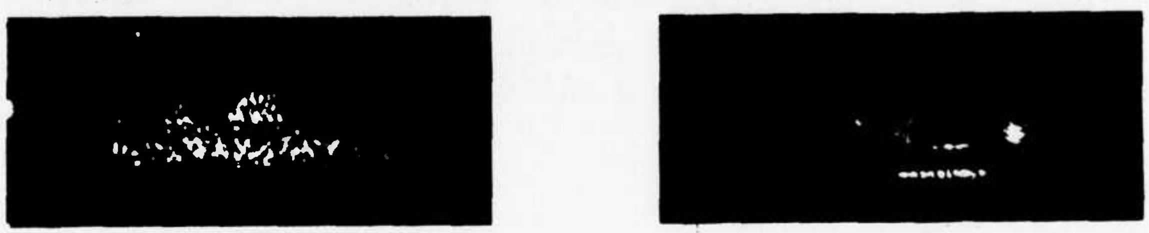

c) 800 λ (equivalent to $\frac{160\ \lambda}{\theta_{subtended}}$)

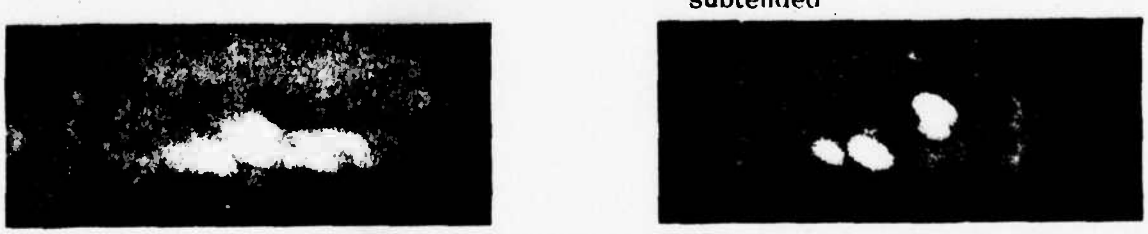

d) 200 λ (equivalent to $\frac{40\ \lambda}{\theta_{subtended}}$)

<u>Diffuse Case</u> <u>Specular Case</u>

Figure 8. Optically Simulated Acoustic Pictures of Submarine

For optical illumination, ground glass type diffusers are often used to view specular objects in order to improve the image. It is not clear that comparable techniques can be carried over into sonar applications, especially long-range sonar, due to practical limitations on equipment size.

A word about 3-dimensional viewing effects is also in order. In the typical optical hologram there is usually an extremely large number of elements in the hologram, far exceeding the number required to reconstruct the desired image. Stated in another way, the hologram itself is much larger, by a large factor, than the area of the pupil of the eye. This quasi-redundancy is responsible for 3-dimensional effects, by thus allowing the observer to "rove" in space, appreciating parallactic effects as he moves. If both eyes intercept the hologram, stereo vision is achieved as well.

It is doubtful whether such an abundance of aperture can be made available in an acoustic viewing system. It is likely that all of the available aperture will be needed for the required resolution and possible image quality improvement as has been discussed. The most efficient parallactic appreciation of depth in such a case is then achieved by coherent focussing over the entire aperture, the limitations of which have been covered earlier in this discussion.

IV. OPTICAL CONFIGURATIONS FOR SONAR PROCESSING

Whether echo-ranging is to be used in a sonar application is often dictated by system requirements. Rather than ask if a given sonar system can be implemented as a holographic system, the proper question may be the more general one of whether the required data processing, whatever it is to be, can be performed with a coherent optical system. When one speaks specifically of a holographic sonar usually one is visualizing a CW system with optical reconstruction or processing.

With the more general question in mind, this section of the discussion will consider various possible coherent optical configurations by which all types of sonar processing may be accomplished.

A. CW HOLOGRAPHIC PROCESSOR

Conceptually, the simplest optical processor for a sound viewing system is a holography system, where the received acoustic information is derived from CW or long pulse radiation. As pointed out in the beginning, several techniques are available to translate the acoustic pattern into an optical modulator. If the traditional sonar hydrophone array is to be used, the reference beam is electronically combined with the signal, square-law detected, and then recorded as the optical transmission of data arranged on a suitable medium. The data is arranged to form a suitably scaled image of the sonar array, and the resulting hologram is viewed directly by the observer, as shown in Figure 9.

This recording differs from an ordinary hologram in that it is sampled, i.e., it is equivalent to viewing the hologram through an array of pinholes, which for some spacings can produce foldovers in the diffraction angles. However, with an array spacing of $\lambda/2$ or less, this is of no consequence.

One problem that must be considered with the holographic technique is the probable mismatch between recording and reconstruction wavelengths.

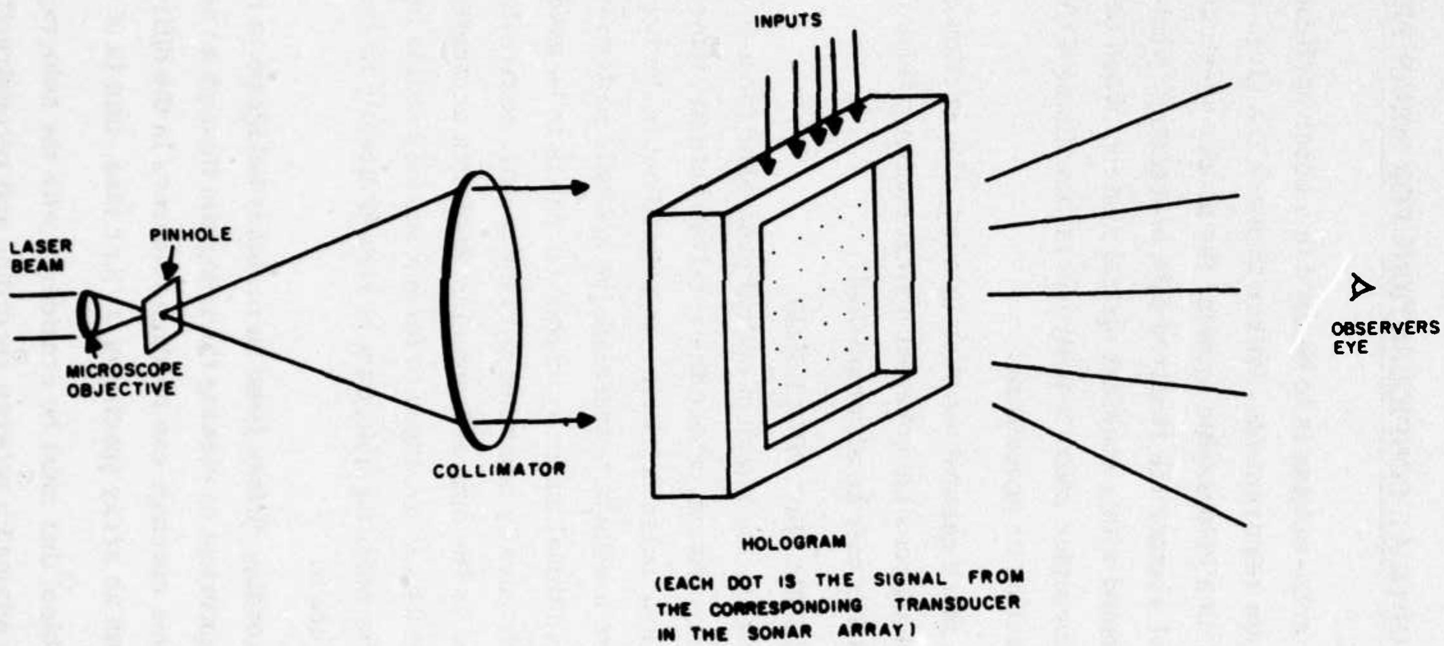

Figure 9. Display of Sonar Hologram

If the sound energy is directly recorded by the optical modulator (method 1 in the Introduction) there is a ratio of λ_o/λ_a

where λ_o = optical wavelength
λ_a = acoustic wavelength

If the output of an array is recorded on the optical modulator as described above, this ratio is arbitrary, depending on the scanning scale.

It is well-known that, theoretically, a holographic reconstruction that is free from aberrations may be produced by scaling the size of the hologram from its original size by the ratio of wavelengths. The aberrations referred to here are both geometric (relative lateral and longitudinal magnification) and optical (such as spherical aberration). Thus one obvious practice would be to scale the recorded hologram to the proper size on the optical modulator. Thus if the element spacing were $\lambda_a/2$ in the sonar array, the element spacing would become $\lambda_o/2$ in the optical domain. This may be very impractical to carry out due to the very small size.

Alternatively, one can correct these aberrations optically by operating only on the diffracted reconstruction beam. The requirement is to map the plane that contains the incorrectly scaled hologram, into a demagnified image plane, preserving amplitude and phase in the new plane. The lenses are thus only required to operate on the diffracted beam. That is, their resolution must be sufficient only to resolve the image modulation, not the fringes in the hologram.

Figure 10a shows the proper arrangement. It is assumed that L1 and L2 are diffraction-limited thin lenses. Elementary geometrical theory shows that all rays shown in dashed lines in the figure have the same optical path length from plane 1 to plane 2, since their common crossover is the focal point for both lenses. These rays are then used to establish equal phase delay from every object point in plane 1, to the corresponding image point in plane 2. The ratio of focal lengths of the lenses, F_1/F_2, determines the magnification of the system from plane 1 to plane 2. Thus if F_1/F_2 is in the same ratio as λ_a/λ_o, and the acoustic hologram taken at λ_a is inserted in plane 1, the reconstruction beam will emerge from plane 2 in exactly the same form as it would have from a correctly demagnified hologram in plane 2. The reconstruction beam emerging from plane 2 is then free of aberrations.

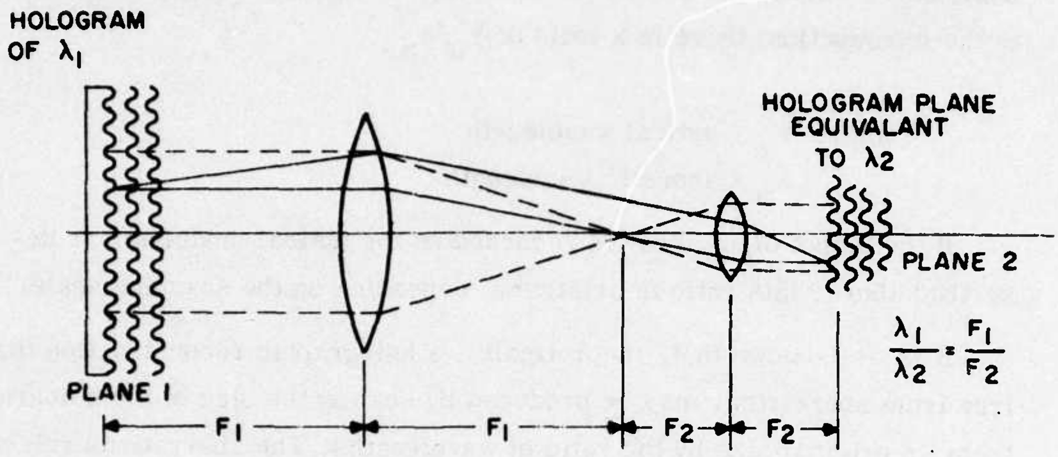

Figure 10a. Correction Optics

The correct planar mapping of optical phase and amplitude from plane 1 to plane 2 can also be appreciated by noting that the crossover or frequency plane is Fourier-transform related to both plane 1 and plane 2.

It is also interesting to note that this cannot be accomplished with a single lens. In Figure 10b is shown such a single lens, adjusted to provide the desired demagnification, b/a, where 1/a + 1/b = 1/F.

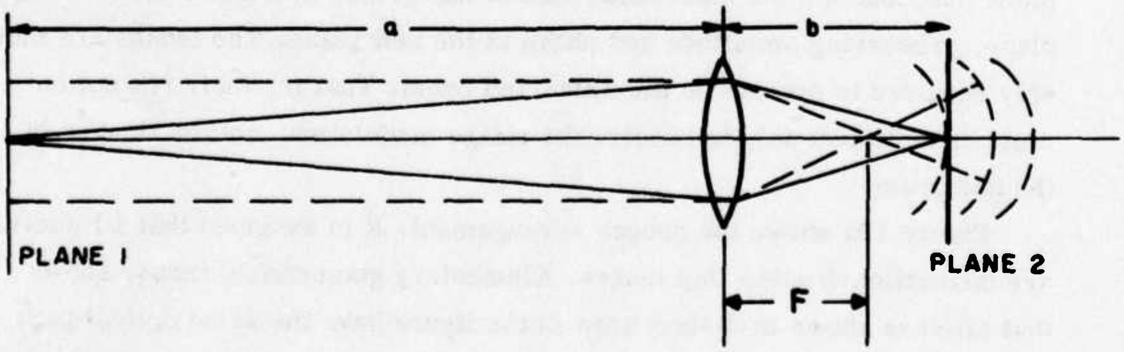

Figure 10b. Single Lens Correction Optics

In this configuration, the rays shown in dashed lines demonstrate that there is a spherical error in phase in plane 2, since the path length from plane 1 to the crossover point, F, is identical for all dashed rays.

In many cases, this latter configuration, while not theoretically perfect, is adequate. Indeed, if axial geometric distortion in the image is of no concern, it will often be satisfactory to diffract light directly from the acoustic

hologram, or from an incorrectly scaled recording of the sonar array. As we have seen in a number of instances, acoustic holograms have been reconstructed properly with a large scale mismatch.

B. MULTICHANNEL CORRELATOR

The previous section dealt with conventional holography in the sense that the output of the optical processor was a recognizable image. More generalized applications of optical processing to sonar are possible where specialized tasks not leading directly to an image can be performed optically. An excellent example of this is the multichannel correlator shown in Figure 11.

One possible application of such a correlator is in detecting the time of arrival of a coded sonar pulse at each element in the transducer array.

Since the transmitted signal is a real time waveform, it can be expressed as the sum of two complex conjugates as follows:

$$S(t) = A(t)\, e^{j[2\pi f_o t + \phi(t)]} + A(t)\, e^{-j[2\pi f_o t + \phi(t)]} \qquad (14)$$

t = time

$S(t)$ = transmitted time waveform

f_o = carrier frequency

$A(t)$ = amplitude modulation

$\phi(t)$ = phase modulation

As shown in the figure, the time signals from each transducer are written as parallel tracks on a moving strip of film. (Photographic film is assumed here, although other media can be used.) Each track corresponds to a separate element in the array, with the time history being displayed as variations in optical transmission along the length of the track. The signals may be recorded directly as received from the transducer, or they may be mixed down to a lower IF, if desired. Since the signal out of the transducer has both positive and negative values, and the recorded optical transmission can have only positive values, it is necessary to add a DC bias to the transducer signal such that the combination is always positive.

This signal experiences a time delay in going to the target and back to element n in the receiving array. If the target is moving, a possible doppler

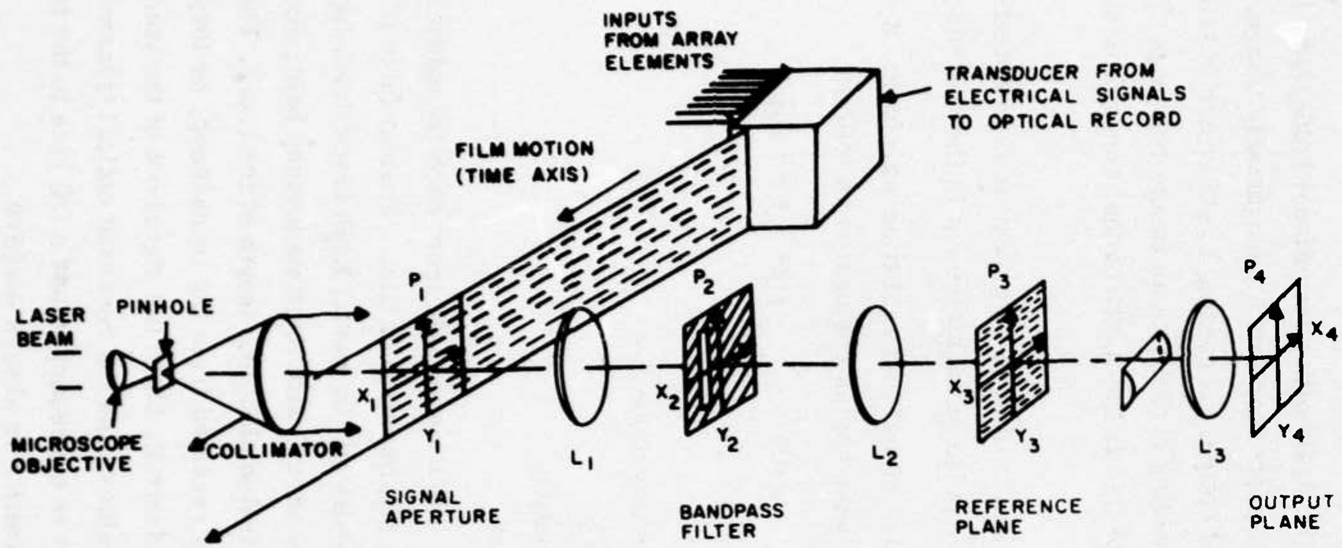

Figure 11. Multichannel Optical Correlator

frequency shift is also experienced. The resulting transmission of track n at position x_1 and time t can be obtained from the following expression:

$$g_1(n,t,x_1) = G_o \begin{bmatrix} B + g_o(t-T_n + \frac{x_1}{V})\, e^{j2\pi f_d(t-T_N + \frac{x_1}{V})} \\ + g_o^*(t-T_n + \frac{x_1}{V})\, e^{-j2\pi f_d(t-T_N + \frac{x_1}{V})} \end{bmatrix} \tag{15}$$

$$\left.\begin{array}{l} g_o(t) = A(t)\, e^{j[2\pi f_o t + \phi(t)]} \\ g_o^*(t) = \text{complex conjugate of } g_o(t) \end{array}\right\} \tag{15a}$$

$g_1(n,t,x)$ = Optical transmission of track n at time t and position x_1.

B = Bias added to electronic signal to insure a positive result.

G_o = Conversion constant to convert electronic signal to optical transmission.

T_n = Time delay for signal to propagate to target and back to element n.

V = Velocity of moving film through processing aperture.

x_1 = Ordinate along time history direction of film (see Figure 11).

f_d = Increase in carrier frequency due to doppler shift.

This recorded time history is transported by the moving film into an aperture where it is illuminated by a collimated beam (plane wave fronts) of coherent light. The aperture is long enough to contain one pulse along its time history direction, and wide enough to contain all of the parallel tracks in the other direction. This input aperture is in the focal plane of lens L_1. It is well established that the complex light distributions (amplitude and phase) which exist at the front and back focal planes of a lens are Fourier transforms of each other. (See Reference 4.) Thus the frequency spectrum of the sonar pulse is displayed along the x direction in the focal plane P_2.

A bandpass filter consisting of an open aperture in an opaque card is used to pass just the frequencies of interest. The lens L_2 takes another Fourier transform, yielding an inverted and filtered image of the input aperture at plane P_3.

The effect of the bandpass filter in plane P_2 is to pass just one of the terms in the previous expression for g_1. Taking this into account, the

expression for the light distribution which illuminates the reference mask in plane P_3 is given by the following.

$$g_3(n,t,x_3) = G_o\, g_o\left(t-T_n - \frac{F_1 x_3}{F_2 V}\right) e^{j2\pi f_d\left(t-T_n - \frac{x_3 F_1}{V F_2}\right)} \tag{16}$$

$g_3(n,t,x_3)$ = complex light distribution in plane P_3 at track = n, time = t, and position = x_3

F_1, F_2 = focal lengths of lenses L_1 and L_2 respectively.

Plane P_3 also contains a reference mask which multiplies this inverted image by the reference signal. The reference mask is constant in the y direction and contains the time waveform of the pulse in the x direction.

The effect of a moving target on a reflected propagating wave is a time compression or expansion of the time waveform. If large doppler effects are expected, the reference mask used in this correlator can be made to match the expected compressed or expanded waveform rather than the transmitted waveform. This waveform is a real positive function given by the following expression.

$$g_r(x_3) = G_r\left[B_r + g_o\left(\frac{x_3 F_1}{V F_2}\right) + g_o^*\left(\frac{x_3 F_1}{V F_2}\right)\right] \tag{17}$$

$g_r(x_3)$ = optical transmission of reference mask at x_3

B_r = bias added to function to insure that it is always positive

G_r = conversion constant relating signal to optical transmission

The spherical lens at L_3 takes the Fourier transform of this product of the reference signal and the input signal. A cylindrical lens is added to the spherical lens at L_3. This cylindrical lens has no curvature in the x direction, so it does not alter the output along x. However, it combines with the spherical lens at L_3 to form an image of plane P_3 at P_4 in the y direction only. Thus the output of each transducer appears imaged at a separate y position in plane P_4, while the transform of the cross correlation between the signal out of the transducer and the reference signal appears along the x direction.

The expression for the output in plane P_4 is obtained by multiplying the light distribution g_3 (equation 16) by the optical transmission of the mask g_r (equation 17) and transforming along x_3 to account for the effect of lens L_3.

Equation 15a is substituted in the result. Three terms result from this operation. For typical parameters, they can be shown to be separated into different regions of plane P_4. Only one of these regions is of significance here. The following expression retains this significant term.

$$g_4(n,t,x_4) = G_o G_r \, e^{j2\pi (f_o + f_d)(t-T_n)} \cdot \int A\left(\frac{x_3 F_1}{V F_2}\right) e^{-j\phi\left(\frac{x_3 F_1}{V F_2}\right)} \cdot A\left(t - T_n - \frac{x_3 F_1}{V F_2}\right) e^{-j\phi\left(t - T_n - \frac{x_3 F_1}{V F_2}\right)} \cdot e^{j2\pi\left(\frac{x_4}{F_3 \lambda} - \frac{f_d F_1}{V F_2}\right) x_3} \, dx_3 \tag{18}$$

$g_4(n,t,x_4)$ = complex light distribution in region of interest in plane P_4 at track=n, time=t, and position=x_4

λ = optical wavelength

This result is a complex expression which gives the amplitude and phase of the light in plane P_4. Notice from the exponential factor outside the integral in the right hand side of equation 18 that the phase is varying with time at the doppler shifted carrier frequency. A coherent reference light beam can be added to recover this carrier when necessary, as will be the case in a later consideration.

Also notice the argument of the last exponential factor inside the integral of equation 18. It is evident from this argument that a shift in doppler frequency causes a corresponding shift in the x_4 ordinate of the light distribution. Thus doppler frequency is displayed along the x_4 ordinate according to the following relationship.

$$f_d \Longrightarrow \left(\frac{F_2 V}{F_1 F_3 \lambda}\right) x_4 \tag{19}$$

Consider this integral, (18), as a function of t and x_4 (which is interpreted as doppler frequency according to equation 19). This is the familiar Woodward ambiguity function associated with the modulation of the coded waveform. At a particular doppler ordinate, the value of the integral, as a function of time, is the envelope of the compressed pulse which typically results from a matched filter or correlation detector. Its time width is

inversely related to the bandwidth of the modulation, which determines the limiting range resolution of the waveform. Similarly, the doppler resolution and any range-doppler ambiguity are determined from this integral which depends only on the mathematical nature of the modulation, rather than the optics involved in the system.

Thus, the output of this optical correlator will consist of a dot of light having a short time duration. The position of the dot in the y direction indicates the channel (transducer) to which the output corresponds. The position of the dot in the x direction indicates the doppler shift of the return signal. The time of occurrence of the dot indicates the arrival time of the pulse. The resolution of the arrival time and doppler shift are limited by properties of the transmitted waveform.

C. BEAMFORMER - CORRELATOR

The preceding system may be modified so that signal correlation is performed in one optical coordinate, and beamforming from a linear array may be accomplished in the second coordinate.

The optical beamformer-correlator has as inputs an IF signal from each element in a uniformly space array, and these signals are recorded as before.

This optical record is processed by the system shown in Figure 12. Again, the optical record is continuously moving through an input aperture where it is illuminated with a collimated beam of coherent light. The optical record consists of an array of parallel tracks, each being a time record from a different element in the array. As in the multi-channel correlator, the collimated light which passes through this optical record is processed by a series of three lenses, a spatial filter, and a reference mask. The output exists in the plane P_4. It is again in the form of a single dot of light having a limited time duration. From the x position of this dot, the doppler frequency shift is obtained. From the time of occurrence of this dot, target range is obtained. Now, however, from the y position of the dot, the target direction angle is obtained. Thus, in effect, beamforming is accomplished in this processor by virtue of the lens L_3. The action is simply the process of a spatial spectral analysis performed by that lens, from the array pattern which is imaged in plane P_3. It should be noted that the beams are already

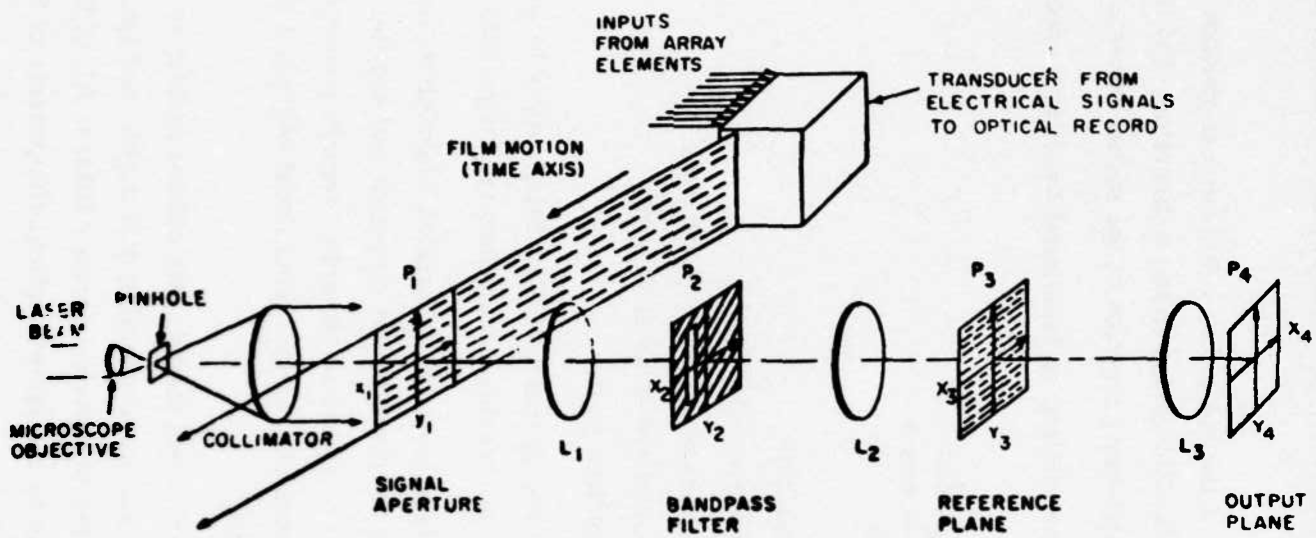

Figure 12. Optical Beamformer-Correlator

resolved in the frequency plane P_2, which information then reimages in plane P_4 in the y coordinate. This beamforming process is equivalent, in one dimension, of course, to the holographic reconstruction previously considered.

The dimension of the dot in the y direction is related to the antenna pattern of the array. The dimension in the x direction, and the time resolution are related to the ambiguity function of the signal waveform.

The following restriction on fractional bandwidth applies to this system.

$$\frac{\Delta f}{f_o} < \frac{1}{\frac{D}{\lambda_a} \cos \theta} \tag{20}$$

Where:

Δf = signal bandwidth

f_o = center frequency of signal

λ_a = signal wavelength at center frequency

D = overall dimension of antenna array

θ = target direction angle

These restrictions on fractional bandwidth apply to any system which uses phase shift beam steering rather than true time delay techniques.

Another important restriction pertains to possible motion of the antenna array. It is assumed that the target direction and doppler frequency with respect to all of the elements in the array remain constant during the duration of the signal being correlated. This could become a serious limitation in some applications.

Within the restrictions stated, this optical system is capable of simultaneously beamforming in all possible directions, and implementing the equivalent of an array of matched doppler filters. All of these tasks are simultaneously done by the simple optical components of three lenses, a spatial filter, and a reference mask.

In this development, it has been assumed that the sonar array is linear, so that beamforming can be mathematically described as a spatial Fourier transform. In many cases it is desirable to use a circular array, which may

provide a more desirable shape, and 360° coverage. The question comes then of whether the Fourier processing provided by optical elements can be used to beamform with a circular array.

We refer here to an important paper by Cheng and Tseng (Reference 6) for the basic answer to this question, with additional information to be found in an article by Sheleg (Reference 7).

Consider Figure 13, in which are shown two concentric rings of transducers in a circular array. A wave arriving at a given angle, θ, is shown. The general philosophy of 3-dimensional arrays is illustrated in this example. To steer the received beam to maximize the reception of this direction, all the various hydrophones are simultaneously phased in relation to each other according to the wavefront diagram shown in Figure 13.

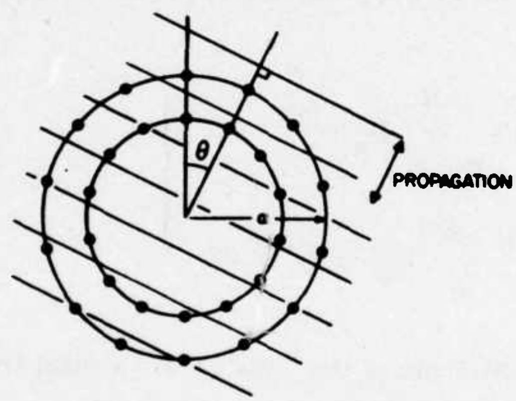

Figure 13. Circular Array

Consider only one ring in the diagram. If all hydrophones are energized in phase, an expanding circular wave is propagated as diagrammed in Figure 14, N = 0. If a linear phase progression is applied so that a 2π phase rotation occurs once around the array, or in 360° physically, an expanding wave will be created with a spiral phase wavefront, as shown in Figure 14, N = 1. If the hydrophones are phased with a 4π progression once around, the wavefront becomes two interleaved spirals, and so forth.

These "modes" retain their identity into the far field. They also represent frequency components of the array excitation, taken along the circular arc, i.e., the array excitation is broken down into a Fourier series, instead of the usual integral, since the pattern is now repetitive.

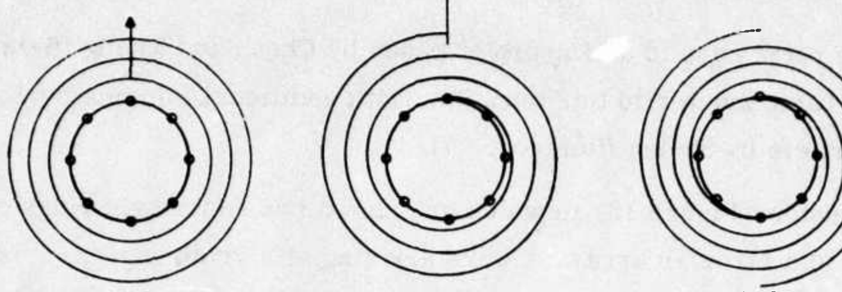

Figure 14. Circular Modes of Propagation

Following the notation of Cheng and Tseng, with a slight modification, the following two Fourier transform pairs may be written to describe the situation:

$$\left.\begin{aligned} E_o(\theta) &= \sum_{n=-N}^{+N} B_n e^{jn\theta} \\ B_n &= \frac{1}{2\pi} \int_o^{2\pi} E_o(\theta)\, e^{-jn\theta}\, d\theta \end{aligned}\right\} \qquad (21)$$

where B_n = coefficients of the "modes" or spatial frequency components
E_o = far field amplitude radiation pattern

In words, B_n is described as the Fourier series decomposition of the far field pattern along a distant arc concentric with the array.

Similarly, a second transform pair may be written interrelating the modes and the aperture function (which is, as opposed to E_o, is discretely distributed):

$$\left.\begin{aligned} A_m &= \frac{1}{M+1} \sum_{n=-N}^{N} C_n e^{jn\theta_m} \\ C_n &= \sum_{m=0}^{M} A_m e^{-jn\theta_m} \end{aligned}\right\} \qquad (22)$$

where $\theta_m = \frac{2\pi m}{M+1}$

$M+1$ = total number of elements

A_m = mth transducer amplitude excitation

C_n = coefficients of spatial frequencies at aperture

Cheng and Tseng show that the C_n's and B_n's are related:

$$C_n = \frac{B_n}{\alpha_n} \tag{23}$$

where

$$\alpha_n = \frac{1}{2\pi} \int_0^{2\pi} g(\theta)\, e^{j\beta a \cos\theta}\, e^{-jn\theta}\, d\theta \tag{24}$$

$g(\theta)$ = the radiation pattern of a single element

β = $2\pi/\lambda_a$

a = array radius

The paper goes on to derive an expression for any $g(\theta)$. In the simple case of isotropic element patterns, α_n reduces to

$$\alpha_n = \frac{1}{2\pi} \int_0^{2\pi} e^{\beta a(\cos\theta - n\theta)}\, d\theta = J_n(\beta_a) \tag{25}$$

where J_n is the nth order Bessel function of the first kind.

We can express equation (25) physically, in words, as follows: When the aperture is observed from the far field, as one tests a particular mode by integration, there is a linear phase progression of $n\theta$ (θ = position on the array) due to the mode being tested, and a sine wave phase modulation, due to the variation in path length to points on the circular array of $\beta a \cos\theta$. Such a combination of linear and sine wave phase modulations mathematically leads to a Bessel progression of weights.

The significant feature of all this with regard to possible optical processing is that the far field pattern is a spatially filtered version of the array function, where the filtering is described by the α_n's in the Fourier domain, as related to both far field and aperture domains. The α_n's are Bessel weights which depend only on the aperture size, and thus are fixed for a

beamforming operation. This is true for non-isotropic elements, as well. Thus the far field and aperture functions are similar domains. This is contrasted to the linear array, where the far field and aperture domains are Fourier-transform related.

Apparently, then, optical beamforming can be accomplished by incorporating one additional lens stage, (after P_4 in Figure 12) to achieve the required Fourier domain of the usual beamformer output for the linear array. A cylindrical lens would be added to prevent any modifications of the temporal information in the x direction. Plane P_4 then becomes the B_n frequency plane, and the α_n weights would be incorporated here.

D. TWO-ANGLE BEAMFORMER-CORRELATOR

It is possible to extend the preceding linear beamforming system so as to multiplex the two angular coordinates, which define the direction in sonar viewing space, into one optical coordinate. We again refer to Figure 12.

In this case, the sonar array is assumed to be two-dimensional, and a recording track in the correlator is provided for each hydrophone in the planar array.

The relative positions of these tracks on the film is significant and are arranged as shown in Figure 15. Notice from the figure that the tracks are arranged in sub-groups. Each sub-group corresponds to antenna elements in a single column on the array. Adjacent tracks on the optical recording are recorded signals from adjacent elements along a column on the array. Similarly, adjacent sub-groups on the optical recording are recorded signals from adjacent columns of elements on the array. On the optical recording (Figure 15), the space between sub-groups is arbitrary. In practice, this space would be minimized.

As before, the plane P_2 is Fourier transform related to the input plane P_1.

In an effort to give some physical insight into how target direction affects this Fourier transform, consider the special case of a square wave signal. Let this square wave be recorded as alternate regions of complete opaqueness and complete transparency on the optical record. Figure 17 shows how the optical recording might look for such a square wave signal.

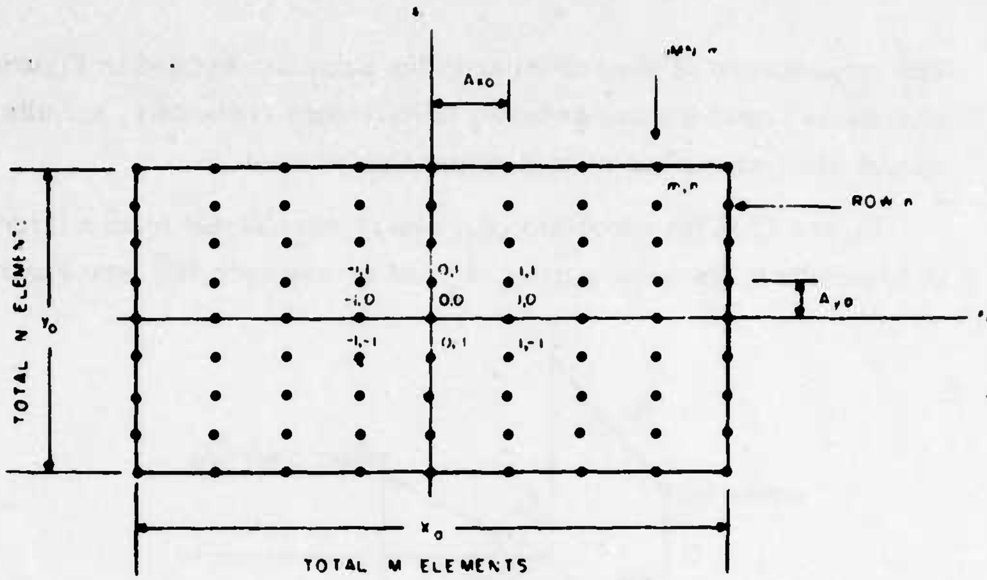

Figure 15a. Planar Array of Discrete Elements or Hydrophones

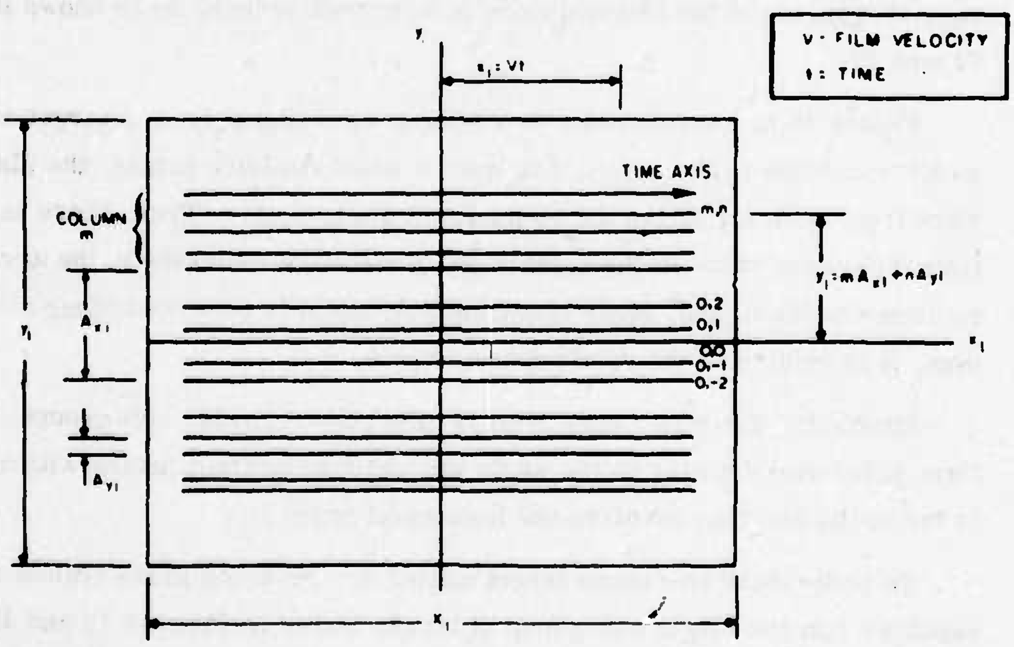

Figure 15b. Optical Recording of Array Output

The array format of the recording is the same as depicted in Figure 15. The continuous signal tracks of Figure 15 have been replaced by the alternate opaque and transparent regions of the square wave.

Figure 17 is the recording of a square wave signal from a target which is broadside to the array, (i.e., θ_x and θ_y are each 90^o, see Figure 16).

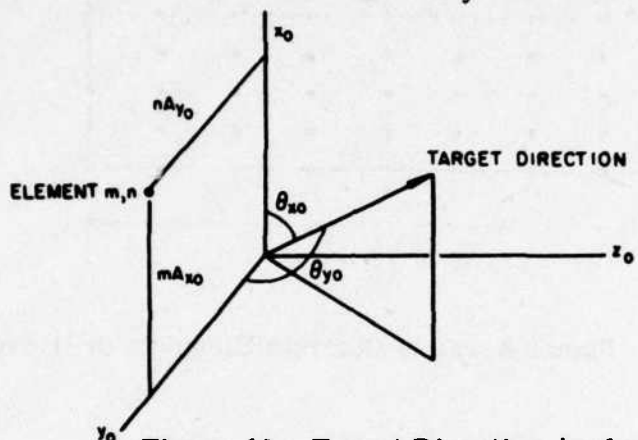

Figure 16. Target Direction Angles

For such a broadside target, each element in the planar array is struck simultaneously by a plane wave front from the target. Thus the square wave signals from all of the elements are in time coincidence, as is shown in Figure 17.

Figure 18 is the recording of a square wave signal from a target which is not broadside to the array. For such a non-broadside target, the plane wave front does not strike all elements simultaneously. Thus, there is a time difference between the signals out of different elements in the array, as shown in the figure. Since this time difference is observed along a column, it is related to the vertical beam angle, θ_y.

Similarly, there is a time shift between the recorded sub-groups. This time difference depends on the angle the plane wave front makes with a row in the array and thus involves the horizontal angle θ_x.

To understand how these target angles are revealed in the transform, consider just the single sub-group of tracks shown in Figures 17 and 18. Here the individual tracks form a close spaced grating of horizontal lines, which cause the light to be diffracted in the vertical direction. The columns of signal periods form a vertical grating which causes light to be diffracted

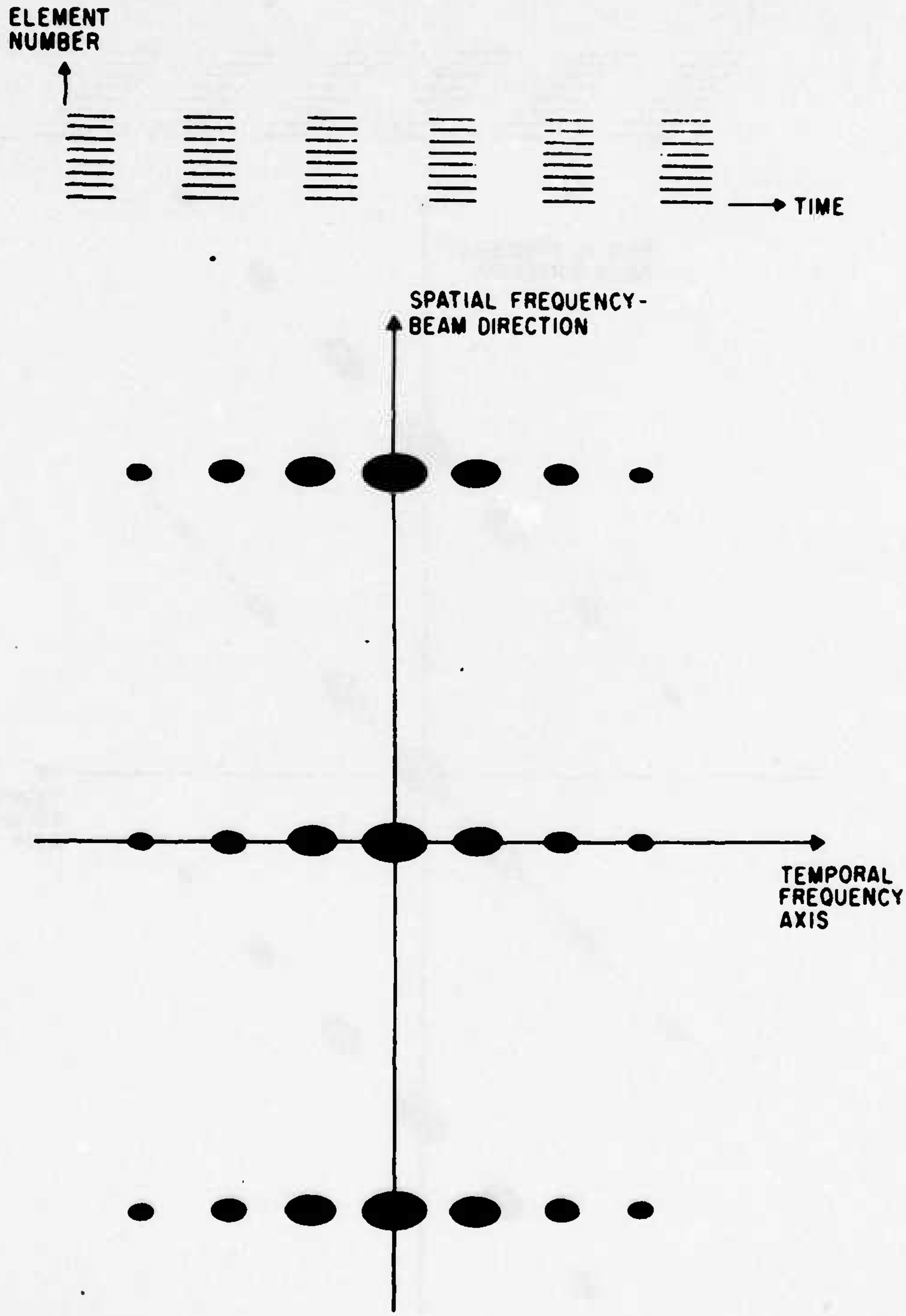

Figure 17. Recording Format for Array Column and Diffraction Pattern - Broadside Target

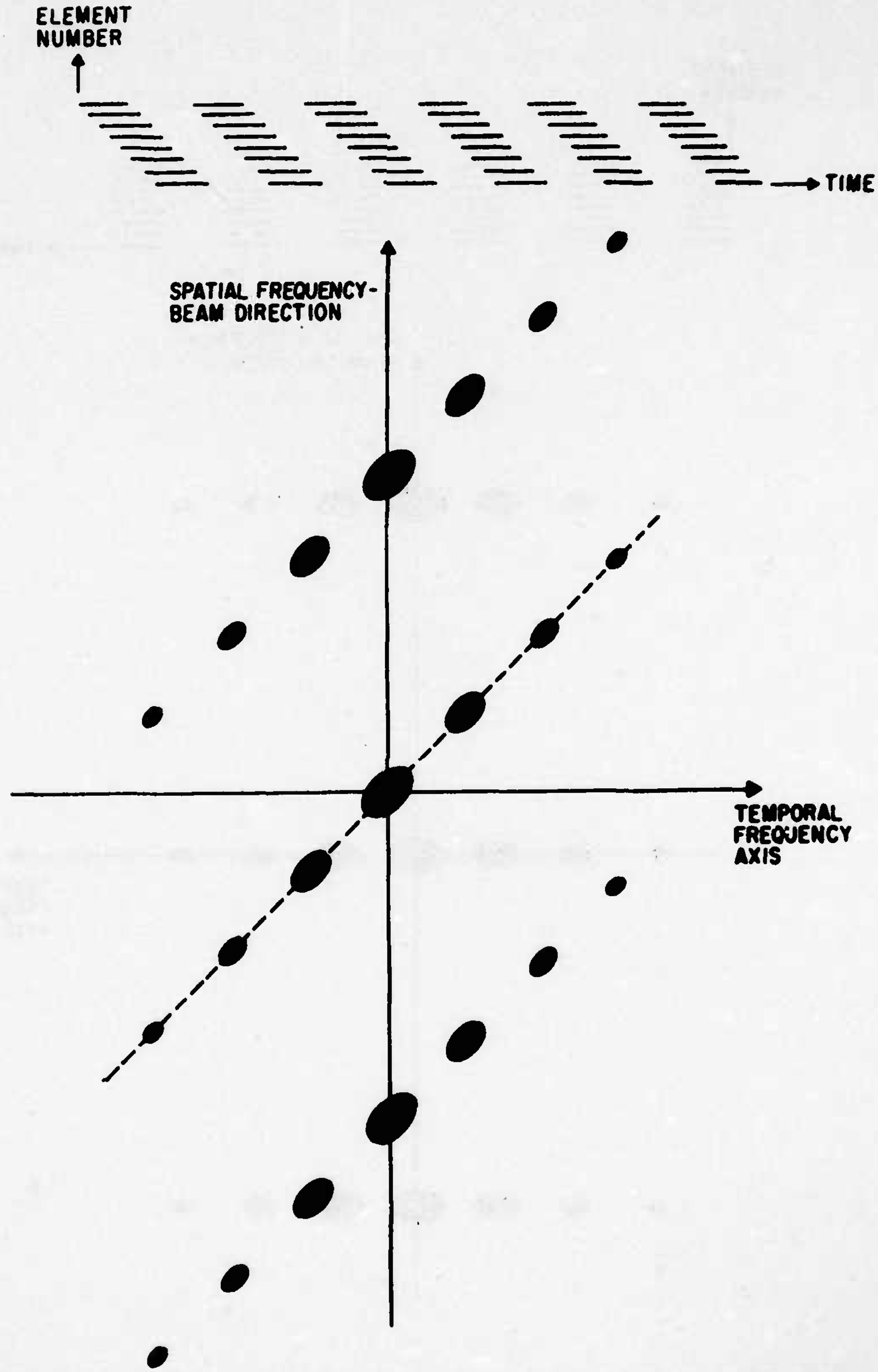

Figure 18. Recording Format for Array Column and Diffraction Pattern - Non-broadside Target

in the horizontal direction. When a non-broadside signal arrives, this vertical grating is tilted an amount which corresponds to the angle of arrival, and the optical diffraction pattern, as shown in Figure 18, changes its direction an equivalent amount (so as to stay perpendicular to the grating).

The resulting diffraction patterns, or transforms, are shown in these same two figures. The vertical repetition of diffraction represents spatial harmonics of the grating formed by the tracks, and the horizontal repetition represents time harmonics of the assumed square wave signal. If the input signal were something other than a square wave, only the relative amplitude of the orders would be changed, but the grid of the pattern and the tilt inherent in the pattern would be the same.

In addition to the close spaced grating created by the tracks, the array format used in the recording causes a coarser horizontal grating which is made of the entire sub-groups. If the fine structure of the individual tracks is disregarded, one can appreciate an overall pattern due to the sub-groups as diagrammed in Figures 19 and 20.

As shown in Figure 20, a non-broadside target again creates a tilt in the vertical grating, but now the tilt is much less for a given element-to-element phase shift (in proportion to the track spacing/sub-group spacing). Again the horizontal repetition in the resulting diffraction patterns are the harmonics of the received time signal, but now the vertical repetition reflects the spatial harmonics of the vertical arrangement of sub-groups.

The slopes of these two different tilts in the diffraction planes are measures of the azimuth and elevation angles of arrival.

In Figure 21, both effects are combined into one composite, which represents the total recording pattern in the multiplexed format, and the resulting diffraction patterns are shown. The overall diffraction pattern becomes the product of the two previously described patterns. The justification of this multiplication must strictly be on the basis of a convolution of recording patterns. To describe the three-fold replication of the pattern shown in Figure 18 into the pattern shown in Figure 20, we would properly think of convolving the former pattern with a column of three impulses, staggered to correspond to the vertical angle of arrival, i.e., staggered to the same tilt as previously described.

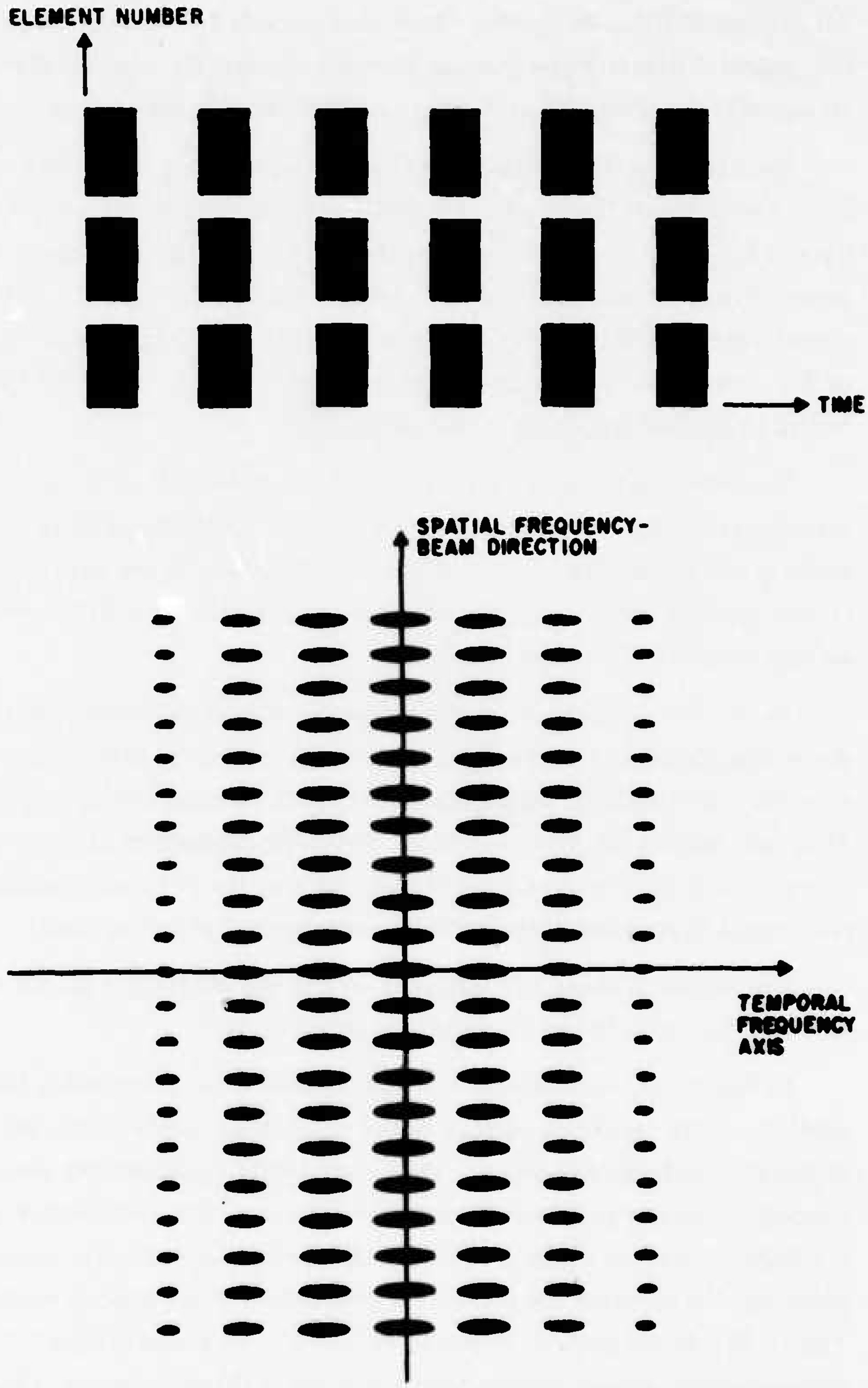

Figure 19. Recording Format for Array Rows and Diffraction Pattern - Broadside Target

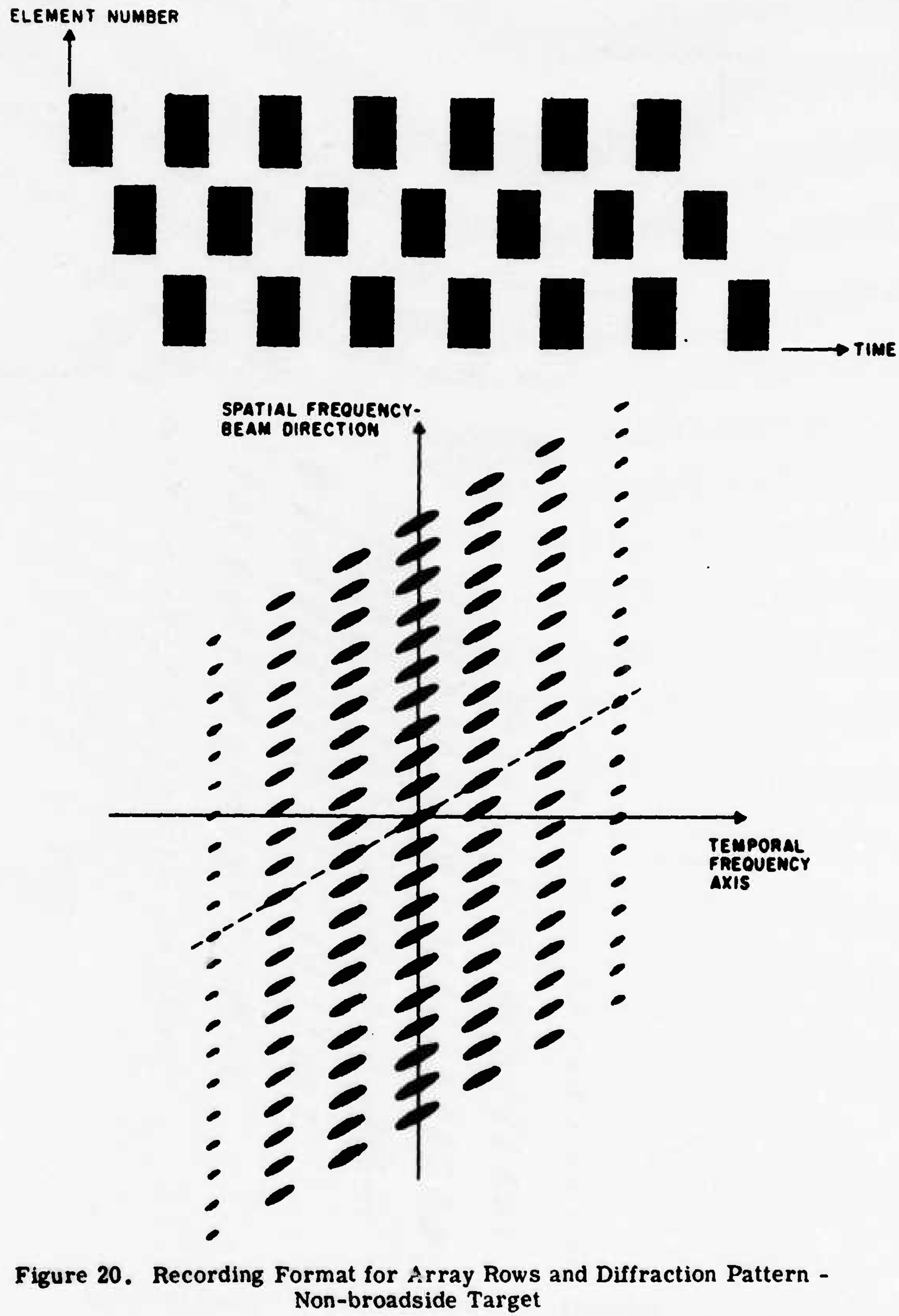

Figure 20. Recording Format for Array Rows and Diffraction Pattern - Non-broadside Target

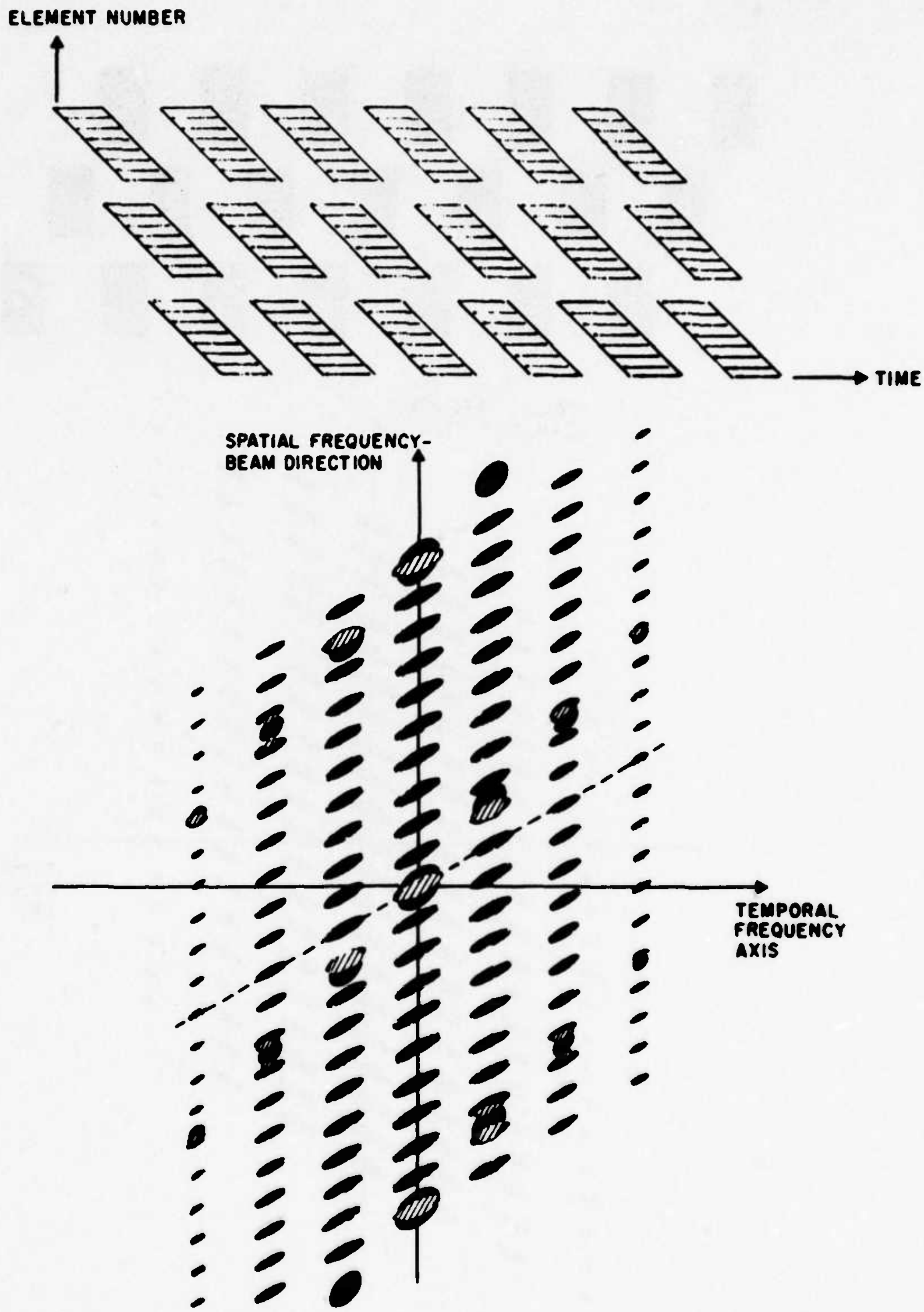

Figure 21. Composite Recording Format for Array and Diffraction Pattern

The target angles are read out within the dotted area shown in Figure 21, where the vertical position of the light pattern in this area indicates both beam angles. This position is measured on a coarse-fine format. To illustrate this more clearly, the readout area is shown on an enlarged scale, for the case of a very narrow band signal, in Figure 22. The x_2 coordinate represents the narrow signal spectrum, and the y_2 coordinate represents the target angles. To the left is shown how the coarse repetitive envelope which represents the target angle θ_y is superimposed on the fine repetitive pattern which represents the target angle θ_x. A succession of three dots is shown, spaced by the fine ambiguity, and within the fine grid any of these can be used to determine θ_x. Their coarse position, taken as a group, represents θ_y.

The output pattern with a wide bandwidth condition is shown on an enlarged scale in Figure 23. The angles of the two component patterns are related to target angles as indicated. The vertical boundaries indicate the (horizontal) extent of signal bandwidth.

For optimum beamforming, the system in the situation of Figure 23, due to the wide bandwidth, would require time-delay steering instead of phase steering. This is reflected in the fact that the three spectral intersections shown (in black) are tilted enough so that they span, vertically, a larger spatial bandwidth than they would for a broadside target, in which case they would be oriented horizontally.

Another feature to be noted in Figure 23, is that the coarse and fine spectral lines do not pass through the optic axis origin as they did in previous examples. This is the general result if the signal is mixed down to an IF band before recording. In the previous examples, it was assumed that the acoustic carrier cycles were directly recorded.

A mathematical treatment of this system with regard to both correlation and beamforming has been prepared and is available from the authors (reference 9). This development assumes an arbitrary signal and formally justifies the patterns which have been heuristically described.

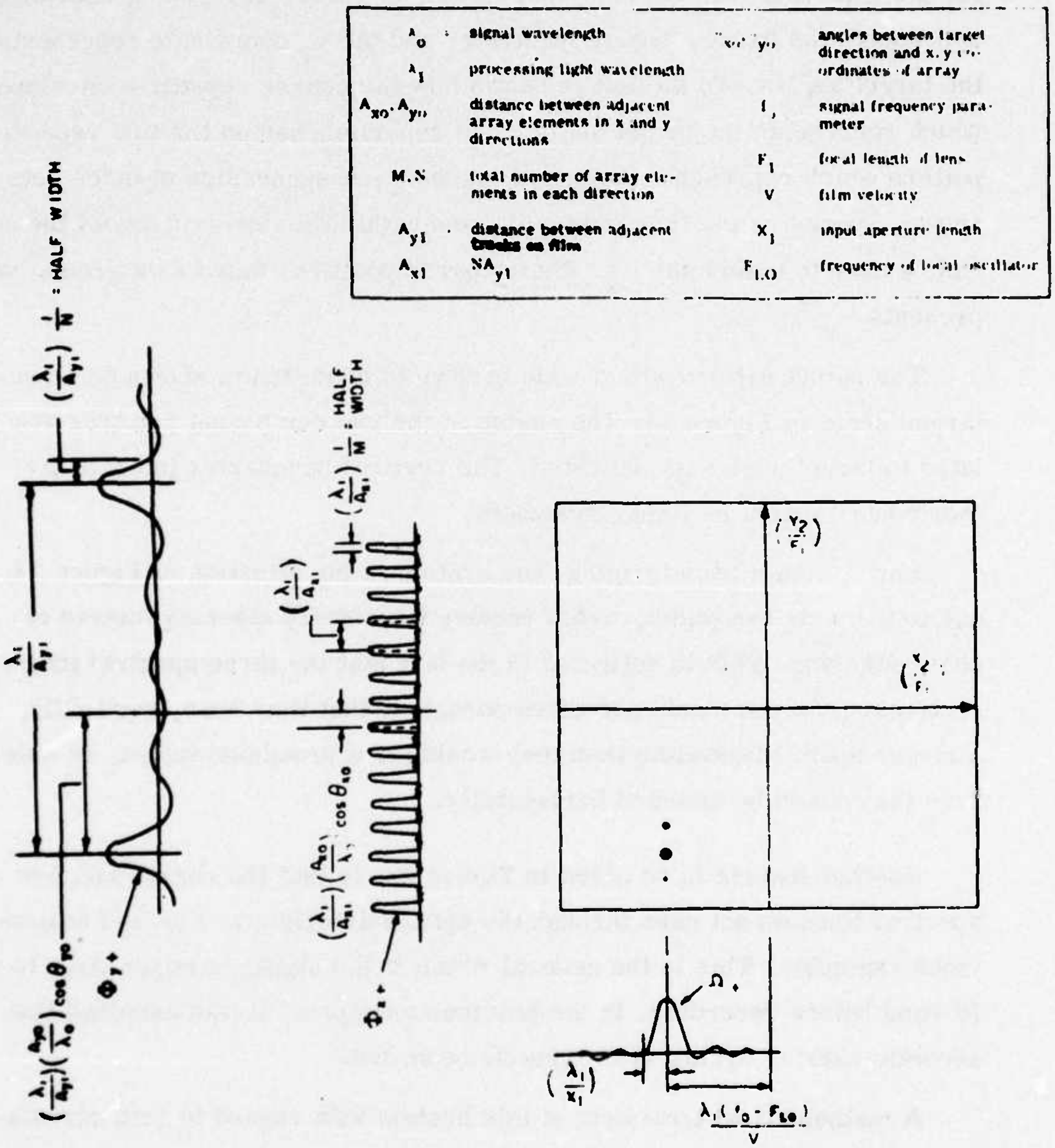

Figure 22. Beamformer Spectral Output for Single Frequency Signal

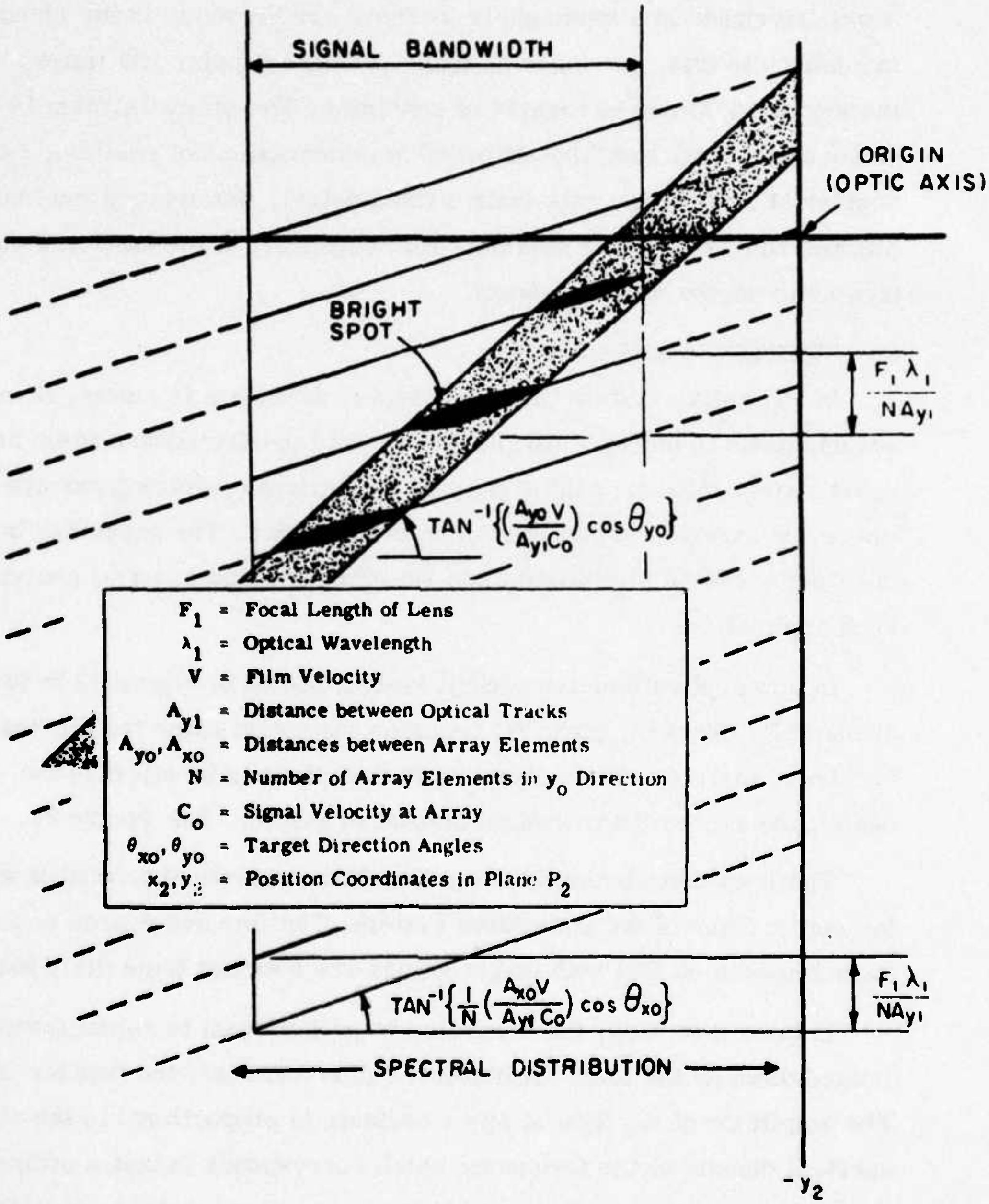

Figure 23. Beamformer-Spectrum Analyzer Output for Wide Band Signal

This discussion has not dealt with hardware problems. However, in view of the enormous quantity of data which can be processed by such a system, hardware problems are expected in transferring data from the array elements to the optical recording and from the output plane to some device which would use this informatoin. That is, there are as many resolvable beam directions in a hemisphere as there are elements in the planar array. In addition to this, there are as many possible doppler and range bins as the signal waveform is capable of resolving. The optical system is capable of simultaneously handling all possible combinations of position, range and doppler at a real time rate (with a fixed delay). However, it may be quite difficult to maintain this high data rate capability at the input and output interfaces with the optical system.

E. SPECTRUM ANALYZER

In any active system where the signal waveform is known, it would be advantageous to incorporate correlation into the detection system as indicated above. However, there may be applications involving passive listening where the expected signal waveform is not known. The preceding beamforming system can be simplified to do beamforming and spectral analysis for such applications.

In this application, the optical system shown in Figure 12 is terminated at plane P_2. That is, plane P_2 becomes the output plane for the beamformer-spectrum analyzer. The system up to this plane is identical to the beamformer-correlator system discussed earlier. See Figure 24.

The light distribution in the y direction is identical to what it was in the output plane of the correlator system. The fine and coarse scales are superimposed so that both target angles are obtained from the y position.

In the x direction, the x position is proportional to signal frequency (mixed down by the local oscillator), rather than only the doppler frequency. The amplitude of the light at any x ordinate is proportional to the signal spectral density at the frequency which corresponds to that x ordinate. Thus the signal spectrum is displayed in the x direction, and target position is indicated in the y direction.

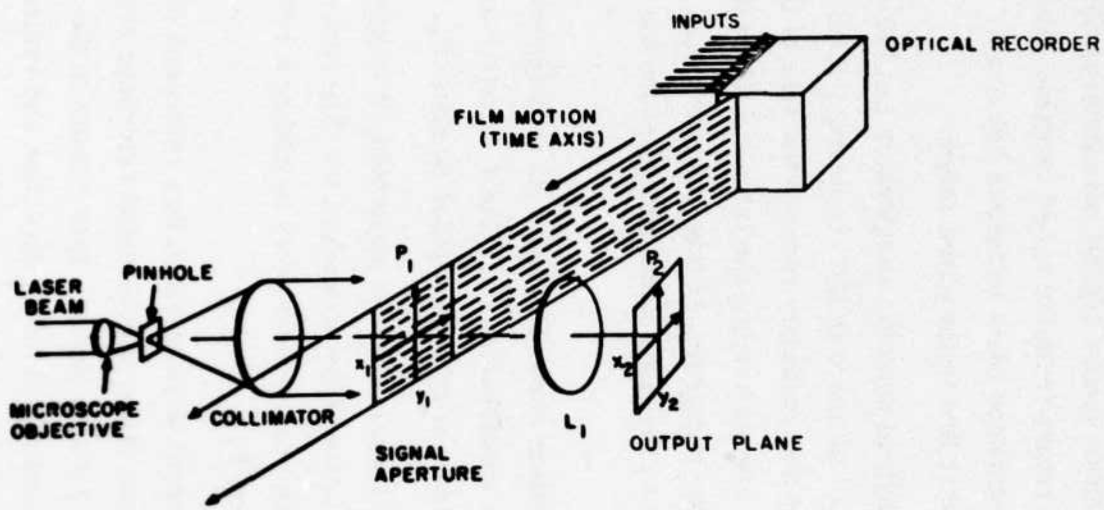

Figure 24. Optical Beamformer-Spectrum Analyzer

F. HYBRID SYSTEM: MULTICHANNEL CORRELATOR WITH HOLOGRAPHIC OUTPUT

Holography, as the term is conventionally used, is a CW method having a range resolution which is limited by aperture size as discussed earlier. On the other hand, conventional sonar uses broadband pulses to obtain much higher range resolution (under typical parameters). A hybrid system is possible in which the return from the target is range gated and electronically combined with a reference beam to form a hologram. The hologram will then reconstruct only what lies in the gated range.

Using such a hybrid system, an operator can initially use a very broad range gate to see all of space in the reconstructed hologram. He then chooses a target of interest and gradually reduces the size of the range gate and controls its position, always keeping the target of interest in the region of space reconstructed by the hologram. In this manner he can reduce the range gate to the size limited by the pulse width and measure the range of any targets of interest.

The hybrid system shown in Figure 25 is based on this idea. Planes P_1 through P_4 form a multichannel correlator, similar to the system discussed before, which yields a compressed pulse at plane P_4.

Since now a hologram is to be generated, it is necessary to recover the carrier and its relative phase in each of the different channels. As mentioned earlier, this carrier can be recovered by adding a reference beam to the light distribution in plane P_4.

There are several ways in which this reference beam can be added. For convenience of illustration, a collimated reference beam tilted in the vertical plane (see Figure 25) was chosen. This results in the reference beam having a phase which is constant in the x_4 direction and varies linearly in the y_4 direction. Assuming that the discrete tracks are uniformly spaced in the y_4 direction, a fixed phase difference exists between adjacent tracks. This phase difference, $\Delta\beta$ is related to the angle of the reference beam and the distance between the tracks. Taking this phase increment into account, the reference beam is given by equation (26).

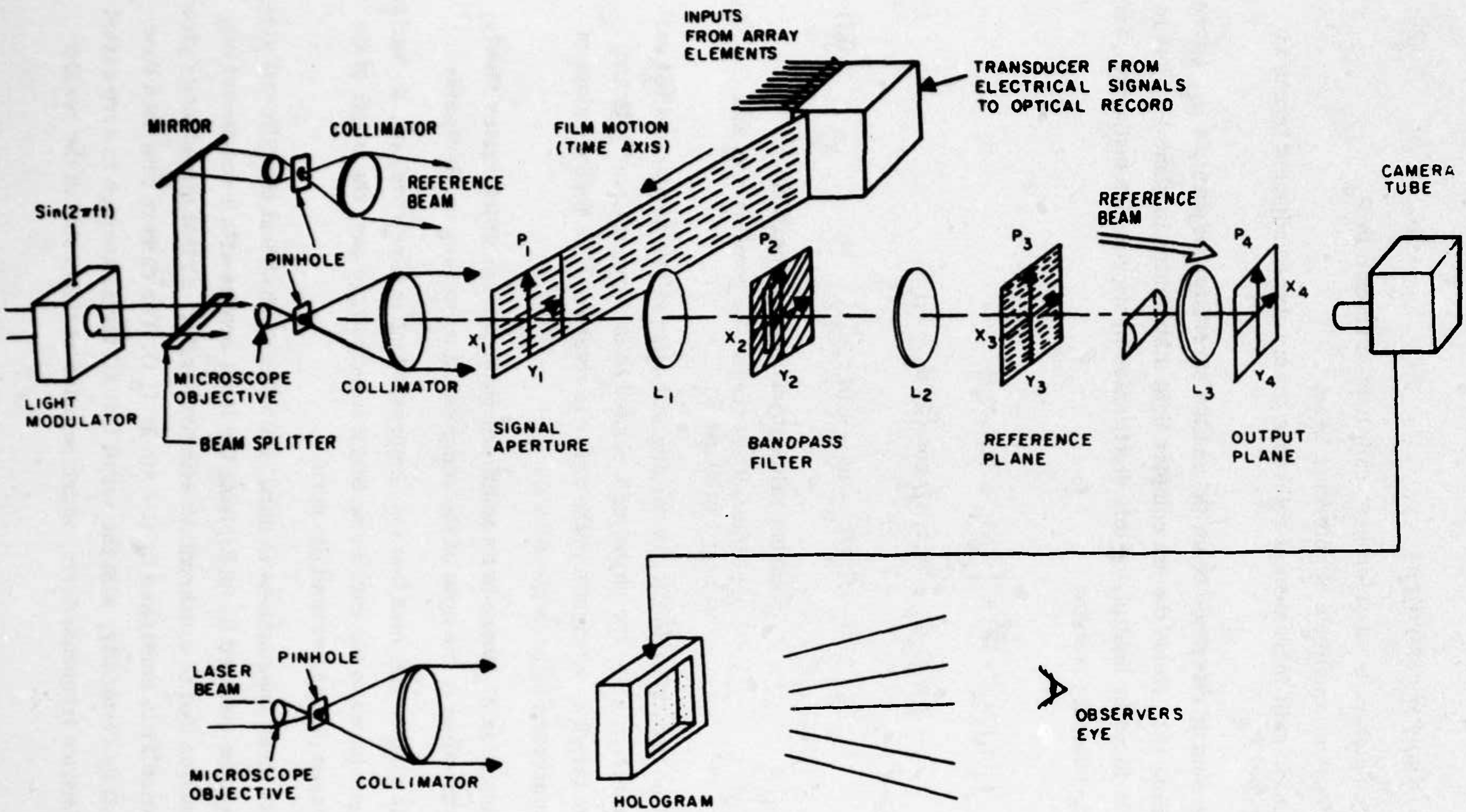

Figure 25. Hybrid Sonar Processor Using Coded Pulse and Hologram Display

$$R(n) = W \exp(j\, n\, \Delta\beta) \tag{26}$$

$R(n)$ = complex value of reference beam light at track n in P_4

W = constant amplitude of reference beam

$\Delta\beta$ = phase shift increment of reference beam between adjacent tracks in plane P_4

The sum of reference beam (R) and the correlator output light g_4, (given by equation 18), yields the net complex light distribution in plane P_4. The intensity is found by multiplying this distribution by its complex conjugate. The following intensity results:

$$\begin{aligned} I_4(n,t,x_4) = W^2 &+ \left[G_o G_r\, \psi(n,t,x_4)\right]^2 \\ &+ 2\, W\, G_o G_r\, \psi(n,t,x_4) \cos\Big\{2\pi (f_o + f_d)\, t \\ &- 2\pi (f_o + f_d)\, T_n - n\beta + \alpha(n,t,x_4)\Big\} \end{aligned} \tag{27}$$

$\psi(n,t,x_4)\, e^{j\,\alpha(n,t,x_4)}$ = complex value of integral in Equation 18.

$I_4(n,t,x_4)$ = light intensity at track = n, position = x_4 and time = t in plane P_4

Notice that this intensity is varying with time at the doppler-shifted carrier frequency; also, the phase shift related to the transit time T_n to and from the target to element n in the array is retained. The time envelope of this compressed pulse is given by ψ.

In equation 27, there is an additional phase term α which varies slowly, so that its effect in the span of the compressed pulse may be disregarded.

It is further assumed that the compressed pulse time envelope, ψ, varies slowly compared to the carrier so that a time average over the length of the compressed pulse is essentially zero.

With these assumptions in mind, the relative phases at the different elements can be obtained by multiplying the laser source with a cosine-varying time function that is synchronized with the carrier, so that the intensity given by equation 27 is multiplied by $(1 + \sin 2\pi\, f_o\, t)$. The camera tube then time-averages this intensity, with the result that all terms average to zero except the difference frequency term, which remains as the cosine of the residue phase.

A hologram is constructed from the data obtained from the camera tube. It consists of an array of dots which form a suitably scaled image of the original array of sonar transducers. Each dot has an optical transmission which is proportional to the time averaged signal from the corresponding channel in the camera tube.

The following expression for this optical transmission results from performing the operations discussed above on I_4 as given by equation 27.

$$H(n) = K_o + K_1 \cos (2\pi\ f_o\ T_n + n\Delta\beta) \tag{28}$$

$H(n)$ = optical transmission of point n in constructed hologram

K_o, K_1 = constants related to amplitude of signal from target and various system parameters present in equation 27

The equations presented in this development imply a single point target. Since the operation of the system is linear, return signals from all points in a continuous scene will be superimposed in the integrating camera tube so that the resulting hologram will reconstruct the complete scene.

Range gating is accomplished by multiplying the laser beam with a pulse superimposed on the cosine varying wave. The time width and location of the pulse determine the size and location of the range increment being reconstructed by the hologram. These are controlled by the operator as discussed earlier.

The angle of the reference beam needed to reconstruct a scene from the hologram is related to $\Delta\beta$ in equation 28. The relative positions of the different tracks on the film is the same as discussed in the section on the beamformer-correlator. Thus there is a linear phase shift increment of $\Delta\beta$ for adjacent elements in a column, and a linear phase shift increment of $M\Delta\beta$ for adjacent columns, where M is the total number of elements in a column of the sonar array. These same linear phase shifts would result if a collimated acoustic reference beam were used at the actual sonar array at the appropriate angles. That is, such an acoustic reference beam angle could be chosen to have a phase shift of $\Delta\beta$ between adjacent elements in a column, and a phase shift of $M\Delta\beta$ between adjacent columns. If such an acoustic reference beam were used, combined with the signal from a point in the scene, and square law detected to determine intensity at each element in the sonar array, a hologram identical to that given by equation 28 would result.

Having generated an acoustic hologram as discussed above, it can be viewed through an appropriate lens system to produce an undistorted scaled scene as discussed earlier.

V. ADDITIONAL OPTICAL ENGINEERING CONSIDERATIONS

A. STORAGE MEDIUM

1. Photographic Film

In any of the optical systems discussed, it is necessary to store the data to be processed on some medium in an aperture where it can spatially modulate the coherent light beam. Photographic film is commonly used for this purpose.

There are several methods for converting the electrical signals to the required optical density variations of the film.

a) The information to be recorded can be displayed as brightness variations on a cathode ray tube, and the tube face is photographed by the film.

b) An electron beam can write directly onto the film.

c) An array of individual light sources, such as light emitting diodes, can be modulated by the electronic signal and photographed by the film.

The use of a CRT is probably the most commonly employed method. Special purpose tubes have been developed for this application. Their face plate consists of an optical fiber bundle with the phosphor on one end of the fiber. The film is in contact with the other end of the fibers during exposure.

If higher resolution is required, the film can be written on directly by an electron beam. This complicates things considerably since the film must be in a vacuum for writing. (In air electron beam writing is possible, but its resolution is not as good as writing in a vacuum.)

If the data rates are too high to multiplex onto a single wire for modulating an electron beam, an array of light emitting diodes might be used. Although large arrays of light emitting diodes have been made, they are not common. Also, driving a large number of elements in parallel requires a large number of wires and associated drive equipment. (Matrix methods can be used to address a large array, but this gets back to time multiplexing and high data rates.)

In real time systems such as the multichannel correlator discussed earlier, the film is continuously moving past the write head (CRT face). The rate at which it moves is related to the highest frequency to be recorded and to the maximum available film resolution. The required brightness of the writing head (CRT face or light emitting diode source) increases as the film velocity increases. Thus, if very high frequencies are to be recorded, sufficient exposure will be a problem.

After exposure to the signal, the moving film passes through the necessary chemical baths to develop the film and prepare it for the processing aperture. Rapid film processors for rugged military environments have been built which have about ten seconds delay between the input electronic signal and the developed film in the aperture of the optical processor. The rapid development is achieved by using very hot developing fluids. To withstand these high temperatures, special hardened emulsions must be used on the photographic film. These special emulsions have a comparatively poor resolution of about 50 to 100 lines per millimeter. (Conventional holograms are made on special high resolution emulsions having several thousand lines per millimeter resolution.)

Another important consideration is the rate at which photographic film is consumed. The velocity with which the film moves is the ratio of the highest frequency to be recorded divided by the maximum resolution of the film. As an example, consider an upper frequency limit of 20 Kc and a film resolution of 50 line pairs per millimeter. This results in a film velocity of 400 mm/sec.

Film costs approximately $50.00 per thousand feet for 35 mm; 70 mm film would cost approximately twice this amount and 16 mm film would be one-half this value. At the previous rate of usage (about 80 ft/min) the film costs about $4/min. for 35 mm film. Thus continuous use is expensive.

Of course, this rate of film usage applies only to systems which process the time waveform, such as the multichannel correlator. Systems which simply display a sampled hologram use film only at a rate necessary to update the hologram. Since the holograms are small and need updating only when the scene changes, film usage could be slight in such systems.

The preceding analyses have assumed that the film modulated only the optical amplitude of the light and did not alter the relative phase across the aperture. This requires that the optical thickness of the film be constant to within a small fraction of an optical wavelength over the entire input aperture. In practice, the film is reasonably flat over a square aperture about 5 mm on a side. As the aperture size is increased beyond this, thickness variations in the film produce noticeable degradations.

When large apertures are necessary, this difficulty can be overcome by submerging the film in a liquid whose index of refraction matches that of the film, which removes any effects of non-flatness. Such a gate has many practical problems associated with it, but it can be used when necessary.

2. Surface Deformable Materials

The analyses assumed that the signals to be processed were stored in the input aperture as variations in amplitude transmission of light. It can be shown that this condition is approximated if phase modulation (small compared to one radian) is used instead of amplitude modulation. Thus modulation of optical thickness rather than optical density is possible.

Three types of surface deformable materials are known for such phase modulation: Oil films, thermoplastic films, and photoplastic films.

A thin oil film is used to coat an optically flat glass disk in a vacuum. An electron beam is used to write on the oil film. The electrons which are deposited on the film are attracted by a high voltage on the glass disk. This force causes deformations in the surface of the oil film, resulting in thickness variations of the film which can be used to phase modulate light passing through the film.

Such a system has several practical problems associated with maintaining the required vacuum in a sealed-off system containing oil. However, such systems have been commercially built for TV projection systems and are practical. They have the advantage that the oil is reusable so that a continuous consumption of photographic film is not necessary. They also do not have the delay associated with the photographic film systems.

Unfortunately, these systems have not yet been applied to coherent optical processing to the same extent as photographic film. Thus development work is necessary in this area especially in regard to the achievable storage time.

Thermoplastic film is very similar to the oil film projector. A thin layer of low melting-point plastic is coated on a transparent conducting film. The film is written on by an electron beam and heated to the softening point of the plastic coating. The electrons are attracted by a high voltage on the conducting backing, and produce thickness variations in a manner similar to that of the oil film. After cooling, the plastic hardens retaining the information written on it. Thus a permanent record is available if desired. The thermoplastic can be erased and reused by heating the plastic and smoothing the surface.

Many of the practical problems associated with the vacuum of the oil film projector also apply to thermoplastic. Military airborne display systems have been built using thermoplastic.

Photoplastic is very similar to thermoplastic. In this case the thermoplastic layer is also a photoconductor. The surface of the photoconductor is charged, and at points where light strikes the photoconductor, the charge leaks through to the conducting layer on the base. The charge which remains on the surface causes deformation when the photoplastic is softened by heating in the same manner as with thermoplastic.

Photoplastic eliminates the troublesome vacuum equipment associated with thermoplastic. However, its sensitivity to light is not as good as photographic film. It has great potential, but presently it is not as well developed as thermoplastic and oil film projectors.

All of these surface deformable techniques have resolution comparable to that of the rapid processed photographic films. They also have the advantage of reusability and no delay time for development. The equipment required to use these techniques at the present time are admittedly complex.

3. Acoustic Delay Lines

Solid materials have the property that their optical index of refraction changes with density. Thus, phase modulation of a coherent light beam can be achieved by an acoustic delay line in which the acoustic pressure provides phase modulation.

The delay line is at the input aperture of the optical processor. The time waveform to be processed is propagated through the delay line (in a system such as the multichannel correlator). The signal propagating through the delay line is an acoustic disturbance consisting of pressure variations. These pressure variations cause an associated change in the local index of refraction, which phase modulates the light passing through it.

This approach has several desirable features such as complete reusability, no delay time for development of film, no vacuum system problems, etc.

The relatively large size of each delay line limits the number of channels which can be processed in parallel by systems such as the multichannel correlator. Some practical problems also exist with the transducers necessary to drive the delay lines, but these problems are not prohibitive.

B. INPUT AND OUTPUT INTERFACES

The main advantage of optical processing is its ability to process large quantities of data in a simple manner. If the input data is of an electrical nature rather than optical, a natural bottleneck exists in converting this input to a suitable optical format. That is, the electronic signals must either be multiplexed into a single channel for conversion to an optical input, or many parallel channels must be provided. The multiplexing approach requires high speed electronic circuitry for large quantities of data, while the parallel channel approach requires more equipment. Once that the data is in a suitable optical format, the optics does parallel processing in a simple manner with few pieces of equipment.

If the output is to be presented in the form of an optical image (holographic output) no output problem exists. However, if the data is to be converted back to electronic signals, the same difficulties in handling large quantities of data electronically arise. These input and output interfaces between electronics and optics are the major areas where problems can be expected.

VI. SUMMARY

Holography, as applied to sonar, is a means of processing the signal from a sonar transducer array to form a visible image of the scene illuminated by the sonar waves. The quality of this image is limited by several theoretical considerations, which also apply to more conventional sonar processing techniques.

This restriction on image quality results mainly from the limited information content of the signal received by the transducer array. In a noisy environment, the maximum total number of resolvable points in the far field of the array is of the same order as the number of independent elements in the array This restriction is fundamental and cannot be circumvented by using a different processing technique, such as holography.

A primary advantage of holography as applied to sonar is its ability to process large quantities of information in an inherently simple manner. This advantage becomes more pronounced as the number of elements in the array is increased. The increased number of elements requires a corresponding increase in the quantity of electronic equipment to process this data in conventional systems, while the holographic system remains essentially unchanged as the array size is increased. The resulting image also improves with increased array size.

Holography is a particular form of the more general field of optical processing. Holography, as popularly used, implies a recognizable image as an output. More generalized operations, such as matched filtering, correlation, spectral analysis, etc., can also be performed by processing techniques. Many of these have applications to sonar processing. In all cases, the optical approach has the advantage of being able to process large quantities of data in an inherently simple manner.

Since the major asset of optical processing is so related to large quantities of data, some difficulties may arise at interfaces between electronic and optical systems. The limit of parallel information which an optical system can handle is related to the sizes of optical elements, and the resolution capability of the storage medium in the input aperture. The rate at which this information can be processed is limited mainly by the rate at which the data in the input aperture can be changed. The electronic equipment to present this data at the input aperture of the optical system can be expected to be the limiting factor on the data rates which can be processed optically. Similarly, the electronic equipment necessary to interface the output of an optical processor with an electronic system can be expected to be the limiting factor on the useful output data rate of an optical system. (Of course, this limitation on output does not apply if the output is an image intended for viewing by a human operator.)

Thus, holography cannot improve upon the displays which can at least theoretically be made available by other means. Holography can simplify the sonar processing systems and make possible larger systems which would be economically impractical using conventional electronic methods.

VII. REFERENCES

1. M. Born, E. Wolf, Principles of Optics, Pergamon Press, 1959.

2. A. Sommerfield, Optics, Academic Press Inc., 1954, pps. 197-201.

3. R.J. Urick, Principles of Underwater Sound for Engineers, McGraw-Hill, 1967.

4. L. Cutrona et al, "Optical Data Processing and Filtering Systems", IRE Transactions on Information Theory, June 1960.

5. R.W. Meier, "Magnification and Third Order Aberrations in Holography" JOSA, Vol. 55, No. 8, Aug. 1965, p. 987.

6. F.I. Tseng, D.K. Cheng, "Pattern Synthesis of Circular Arrays with Many Directive Elements", IEEE Transactions on Antennas and Propagation, Nov. 1968, p. 758.

7. B. Sheleg, "A Matrix-Fed Circular Array for Continuous Scanning" Proc. IEEE, Vol. 56, No. 11, Nov. 1968, p. 2016-2027.

8. W.A. Penn, "Signal Fidelity in Radar Processing", IRE Transactions on Military Electronics, MIL-6, No. 2, April 1962.

9. J.L. Chovan, "Optical Beamformer-Correlator for Planar Antenna Array," General Electric Co. TIS-DF67ELS-45, May 1967.

10. J.L. Chovan, "Holographic Techniques Applied to Sonar", General Electric Co. TIS-R-68ELS-98, Dec. 1968.

ATE

LME